THE JOURNAL OF BIOLOGICAL CHEMISTRY VOL. 290, NO. 42, pp. 25620–25635, October 16, 2015

MYCBP2 Is a Guanosine Exchange Factor for Ran Protein and Determines Its Localization in Neurons of Dorsal Root Ganglia*

Received for publication, February 19, 2015, and in revised form, August 20, 2015 Published, JBC Papers in Press, August 24, 2015, DOI 10.1074/jbc.M115.646901

Angela Dörr, Sandra Pierre, Dong D. Zhang[1], Marina Henke, Sabrina Holland[2], and Klaus Scholich[3]

From the Institut für Klinische Pharmakologie, Pharmazentrum Frankfurt, Klinikum der Goethe-Universität Frankfurt, Frankfurt 60590, Germany

Background: Ran mediates nucleo-cytoplasmic transport and is regulated by the GTPase-activating protein RanGAP1 and the guanine nucleotide exchange factor (GEF) RCC1.
Results: RanGAP1 transports MYCBP2 to the nucleus. MYCBP2 binds to Ran and stimulates nucleotide exchange.
Conclusion: MYCBP2 is a GEF for Ran.
Significance: The finding that besides RCC1 other GEFs for Ran exist reveals a complex regulation of Ran signaling.

The small GTPase Ran coordinates retrograde axonal transport in neurons, spindle assembly during mitosis, and the nucleo-cytoplasmic transport of mRNA. Its localization is tightly regulated by the GTPase-activating protein RanGAP1 and the nuclear guanosine exchange factor (GEF) RCC1. We show that loss of the neuronal E3 ubiquitin ligase MYCBP2 caused the up-regulation of Ran and RanGAP1 in dorsal root ganglia (DRG) under basal conditions and during inflammatory hyperalgesia. SUMOylated RanGAP1 physically interacted with MYCBP2 and inhibited its E3 ubiquitin ligase activity. Stimulation of neurons induced a RanGAP1-dependent translocation of MYCBP2 to the nucleus. In the nucleus of DRG neurons MYCBP2 co-localized with Ran and facilitated through its RCC1-like domain the GDP/GTP exchange of Ran. In accordance with the necessity of a GEF to promote GTP-binding and nuclear export of Ran, the nuclear localization of Ran was strongly increased in MYCBP2-deficient DRGs. The finding that other GEFs for Ran besides RCC1 exist gives new insights in the complexity of the regulation of the Ran signaling pathway.

The small GTPase Ran (1) regulates nuclear transport, organization of the spindle apparatus during mitosis, as well as nuclear envelope and nuclear pore complex reformation during telophase (2–4). According to its activity state, Ran enters in its GDP-bound form or exits in its GTP-bound form to the nucleus, mediating import and export of proteins or mRNA through nuclear pores (5). Compartmentation of its guanosine exchange factor (GEF)[4] regulator of chromosome condensation 1 (RCC1) and its GTPase-activating protein (GAP) RanGAP1 causes an asymmetric distribution of GTP- and GDP-bound Ran across the nuclear envelope (1, 6, 7). In nondividing cells, RCC1 is located within the nucleus, whereas RanGAP1 is located in the cytoplasm and translocates after covalent binding to small ubiquitin-like modifier 1 (SUMO1) to the cytosolic membrane of the nuclear pore complex (8, 9). In neurons of the sciatic nerve, the Ran/RanGAP1 system is also involved in the regulation of retrograde transport after traumatic nerve injury (10). Because of the necessity of the presence of a cytoplasmic GEF for Ran for this retrograde transport, the existence of a cytoplasmic GEF for Ran, other than the nuclear RCC1, has been postulated (11).

Myc-binding protein 2 (MYCBP2) is an unusually large protein with a predicted molecular mass of 510 kDa. MYCBP2 orthologs, which are summarized as PHR proteins, have been described in humans (PAM), mice (Phr1), zebrafish (Esrom), *Drosophila* (Highwire), and *Caenorhabditis elegans* (RPM-1). Although MYCBP2 is found in many human tissues, its expression is especially high in peripheral and central neurons (12–14) where it inhibits neurite outgrowth, synaptic growth, and synaptogenesis (15–19). Some functions of MYCBP2 depend on its ubiquitin ligase activity such as the inhibition of the p38 signaling pathway through DLK1 or the activation of the mammalian target of rapamycin pathway through TSC2 (17, 20–23). Other signaling pathways are regulated by MYCBP2 independently of its ubiquitin ligase activity. These include the regulation of GLO-4, a GEF for the small GTPase Rab (24), and its GEF activity for Rheb (25). Also, inhibition of adenylyl cyclases by MYCBP2 and activation of the KCC2 ion channel are mediated by its N-terminal RCC1-like domain and are seemingly independent of its ubiquitin ligase activity (26–28).

Here, we report that MYCBP2 interacts with Ran and RanGAP1 and increases the GTP binding of Ran through its RCC1-like domain. MYCBP2 co-localized with Ran in the nuclei of DRG neurons, and genetic deletion of MYCBP2 caused the accumulation of Ran in nuclei, underlining the necessity of the GEF activity of MYCBP2 for the nuclear export of Ran.

Experimental Procedures

Materials—If not indicated otherwise all chemicals were purchased from Sigma, and cell culture media and supplements were from Invitrogen.

* This work was supported by German Research Association (DFG) Grants SCHO817/3 and SFB1039-TP08. The authors declare that they have no conflicts of interest with the contents of this article.
[1] Present address: 3rd Hospital, Hebei Medical University, Shijiazhuang, Hebei 050051, China.
[2] Present address: Shriners Hospitals Pediatric Research Center, Temple University School of Medicine, Philadelphia, PA 19140.
[3] To whom correspondence should be addressed. Tel.: 49-69-6301-83103; Fax: 49-69-6301-83778; E-mail: scholich@em.uni-frankfurt.de.
[4] The abbreviations used are: GEF, guanosine exchange factor; DRG, dorsal root ganglia; GAP, GTPase-activating protein; SUMO1, small ubiquitin-like modifier 1; ANOVA, analysis of variance; GTPγS, guanosine 5′-3-*O*-(thio)triphosphate; mant, *N*-methylanthraniloyl.

Antibodies and siRNA—Antibodies against RanGAP1 (N-19), HSP 90 (F-8), and HSC 70 (K-19) were from Santa Cruz Biotechnology; against SUMO1, His tags were from Sigma, ERK1/2 was from Promega, and Ran (clone 20) was from BD Transduction Laboratories. siRNA was purchased from Dharmacon (Schwerte, Germany). For control, the siRNA pool was as follows: 5′-UAA GGC UAU GAA GAG AUA C-3′; 5′-AUG UAU UGG CCU GUA UUA G-3′; 5′-AUG AAC GUG AAU UGC UCA A-3′; 5′-UGG UUU ACA UGU CGA CUA A-3′. For mouse RanGAP1, the siRNA-SMARTpool was as follows: 5′-GAACGGAAUUAACCAUCCU-3′, 5′-CCACAUGGUCUGCUCAAG-3′; 5′-GGGAUGACGCCUCAGUAAA-3′; 5′-CCUCGAAGCUCUACGAUUG-3′. For human RanGAP1, the siRNA-SMARTpool was as follows: 5′-GACCGAAUGUCACCGGAAA-3′; 5′-GAGAAGAAGUCGGAGUUGA-3′; 5′-UAAAGGAGCUGAACUUGUC-3′; 5′-GAAACCGUCUGGAGAAUGA-3′.

Animals—C57BL/6N mice were supplied by Janvier (Le Genest, France). Conditional MYCBP2$^{fl/fl}$ mice were on C57BL/6N background (20) and were compared with age- and sex-matched Cre recombinase-deficient mice. In all experiments, the ethics guidelines for investigations in conscious animals were followed, and the procedures were approved by the local Ethics Committee.

Immunoprecipitation—Antibody-conjugated beads were prepared by incubation of 30 μl of AG-agarose with 1 μg of antibodies against SUMO1, MYCBP2, Ran, or an unrelated IgG antibody for 1 h at 4 °C in 0.5 ml of PBS. The beads were pelleted (2 s, 4 °C, 1000 × *g*), and the supernatant was replaced by 1 ml of IP-buffer (1% Triton X-100, 50 mM Tris/HCl, pH 7.4, 300 mM NaCl, 5 mM EDTA, 0.02% NaN_3). Cell lysates were precleared by incubation with 30 μl of 50% AG-agarose for 30 min at 4 °C. The beads were removed by centrifugation (5 min, 4 °C, 16,000 × *g*). 500 μg of the precleared cell lysate were added to the antibody-conjugated beads and incubated for 2 h at 4 °C. The beads were pelleted (5 s, 4 °C, 16,000 × *g*) and washed three times with IP-buffer. For Western blot analysis, 30 μl of hot 4× Lämmli buffer were added (29).

Pulldown Assay—Purified MYCBP2 (100 ng), the RCC1-like domain of MYCBP2 (100 ng), or RCC1 (100 ng) were incubated with His-Ran, Ran T24N, or Ran Q69L for 15 min on ice. IP-buffer was added, and the proteins were precipitated with nickel-agarose beads (MYCBP2) or Ran antibody-conjugated AG-agarose beads (4 h, 4 °C). The beads were pelleted (5 s, 4 °C, 16,000 × *g*) and washed three times with IP-buffer. For Western blot analysis, 30 μl of hot 4× Lämmli buffer were added.

Primary DRG Cultures—For DRG primary cultures, 20–30 DRGs were prepared from adult mice and cultivated as described previously (20). The cells were plated on poly-L-lysine-coated coverslips in neurobasal medium containing B27, 2 mM glutamine, 0.1% gentamycin, and 1% penicillin/streptomycin. After 4 days, the cultures were used for immunocytochemistry.

Protein Expression and Purification—Full-length MYCBP2 was purified as described previously (12, 28, 30). Purity was determined using Coomassie-stained SDS-PAGE and activity by autoubiquitylation. His-tagged human RCC1-like domain from MYCBP2 was expressed and purified as published previously (28). An inactive RCC1-LD mutant was generated by substitution of His-912 and His-913 with alanine (26) in the TrcHisB (Invitrogen) vector using site-directed mutagenesis with primers AGC TGT GGA TTT GCC GCT TCA GTG GTT TTA and TA AAA CCA CTG AAG CGG CAA ATC CAC AGC T according to the QuikChange site-directed mutagenesis protocol and purified like the active form. His-tagged human Myc-binding domain (amino acids 2412–2710) from MYCBP2 was expressed and purified as published previously (30). The plasmid for the expression of recombinant Ran was kindly provided by Prof. Dr. F. Melchior, DKFZ-ZMBH, Heidelberg, Germany. Recombinant Ran and RanGAP1 were expressed and purified as described previously (8, 32). Human RanGAP1 in pET23a and human pDsRed1-N1 RanGAP1 were obtained from addgene.org. Ran mutants were generated in the TrcHisB (Invitrogen) vector using site-directed mutagenesis with primers GGT GGT ACT GGA AAA AAC ACC TTC GTG AAA CGT and ACG TTT CAC GAA GGT GTT TTT TCC AGT ACC ACC for T24N and primers TGG GAC ACA GCC GGC CTG GAG AAA TTC GGT GGA and TCC ACC GAA TTT CTC CTG GCC GGC TGT GTC CCA for Q69L according to the QuikChange site-directed mutagenesis protocol (33). Recombinant RCC1 (pPB-C-His) was obtained from Applied Biological Materials (ABM) Inc., Richmond, British Columbia, Canada, and purified as described previously (34). The purity of recombinant proteins was determined using Coomassie-stained SDS-PAGE and their activity by GTPase activity.

In Vitro SUMOylation and Ubiquitylation—*In vitro* SUMOylation of 15 μg of purified RanGAP1 was performed using the SUMOylation kit (Enzo Life Sciences) according to the manufacturer's instructions. *In vitro* ubiquitylation assays were performed in 40 mM Tris, pH 7.4, 8.5 mM $MgCl_2$, 5 mM ATP, 1.5 mM DTT, 10 mM creatine phosphate, 3.5 units/ml creatine phosphate kinase, 50 nM rabbit E1 (Calbiochem), 750 nM E2 UbcH5c proteins (Boston Biochemicals), and 0.2 μg/μl His-ubiquitin (Sigma) as described previously (25). In the absence or presence of full-length MYCBP2 (100 nM), SUMOylated RanGAP1 (5 or 1–10 μg), unmodified RanGAP1 (5 or 1–10 μg), or Ran proteins (5 μg) were incubated for 90 min at 27 °C. To determine MYCBP2-dependent TSC2 degradation, HeLa lysate (20 μg) was added to the assay. The reaction was terminated by addition of gel loading buffer, and the samples were analyzed by Western blot analysis.

Immunostaining of Tissues and Cells—The staining protocol was the same for tissues and DRG cultures. DRGs were taken from untreated mice or after zymosan injection (20 μl, 12.5 mg/ml) in one hind paw at the indicated times. DRGs were placed in tissue TEK O.C.T freezing compound (Sakura Finetek) and frozen in liquid nitrogen. Afterward, cryosections of 10 μm thickness were prepared using the cryotome Leica CM3050S (Leica). The tissue or the cells were fixed in 4% paraformaldehyde in PBS, permeabilized with 0.1% Triton in PBS, and blocked with 3% BSA in PBS-T (0.1% Tween) for 1 h at room temperature. The samples were incubated for 1 h with antibodies against Ran or MYCBP2, followed by incubation with fluorescence-labeled secondary antibodies. Nuclei were stained with DAPI (1 μg/ml, 5 min, room temperature). Background was reduced using Sudan staining (0.6% Sudan BlackB in 70% ethanol, 5 min, room temperature). For all images, an

AxioOberserverZ1 microscope with an AxioCam and standard DAPI, GFP, and DsRed filters were used. Images were taken with a ×40 objective with a resulting resolution of 1388 × 1040 pixels, except for Fig. 8*A*, where the images were taken with a ×63 objective with the same pixel number. Three-dimensional reconstruction of image stacks from fluorescence images was performed using Imaris 7.61 with a set surface grain size of 0.2 μm.

Determination of Protein Translocation and Expression—The cellular localization of MYCBP2, RanGAP1, or Ran was assessed as described previously (20). The experimenter was unaware of the treatment. Briefly, images of about 30 cells per treatment condition from at least three independent experiments were taken, and localization was assessed by generating densitometric line profiles of the cytosolic and nuclear compartments of cells using ImageJ 1.48 software (National Institutes of Health). Primary neurons were judged as translocation-positive if the signal strength for MYCBP2 was in the nuclear region (as determined by DAPI staining), and at least 150% of the signal strength was in the cytosolic region. Cells were judged as translocation-positive for RanGAP1 if the signal strength in the nucleus was at least 250% of the signal strength in the cytosolic region. For Ran, an average nuclei/cytosol ratio was determined according to the same procedure and compared between wild type and knock-out mice.

RanGAP1 expression in siRNA-transfected neurons was determined in comparison with DAPI staining. Images of about 30 cells per treatment condition (transfected *versus* untransfected) from at least three independent experiments were taken under the same conditions and processed with the automatic minimum/maximum correction of the Zeiss AxioVision LE software. Then line profiles of the DAPI staining and RanGAP1 staining were generated with the ImageJ 1.48 (National Institutes of Health) software. The ratio between RanGAP1 and DAPI was determined and compared between siRNA-transfected and -untransfected cells.

Nuclei Isolation—Nuclei isolation was performed according to the manufacturer's instructions (Nuclei EZ prep; Sigma) using confluent HeLa cells. After reaching confluence, the medium was replaced by serum-free medium, and the next day cells were treated with 10% serum for 30 min. The cells were placed on ice, and the nuclei were separated from the cytosol according to manufacturer's instructions. The nuclei were lysed according to Zou *et al.* (35) in nuclear envelope lysis buffer containing 20 mM Hepes/KOH, pH 8.0, 1.5 mM $MgCl_2$, 25% glycerol, 420 mM NaCl, 0.2 mM EDTA, 1 mM DTT, and protease inhibitors.

siRNA Transfection—The transfection was performed with siPORTamine according to the manufacturer's instructions. Primary DRG neurons were cultured for 4 days in neurobasal medium with B27. siPORTamine (5 μl) was diluted in 100 μl of neurobasal medium and incubated for 10 min at room temperature. 6-Carboxyfluorescein-labeled nontargeting siRNA (Life Technologies, Inc.) or SMARTpool siRNA to murine RanGAP1 (Dharmacon) with 1/10 nontargeting siRNA was diluted in medium for a final concentration of 50 nM (stock, 50 μM). The dilutions were mixed, incubated another 10 min at room temperature, and added to the cells. After 24 h, the medium was changed, and after 48 h, the cells were stimulated with 10% serum. Following 3 h of incubation at 37 °C, the cells were washed with PBS and were used for immunocytochemistry. To rescue RanGAP1 expression, cells were transfected with siRNA and simultaneously transfected with plasmid DNA of pDsRed1-N1 RanGAP1 (Addgene). 4 μg of DNA were mixed with 6 μl of TurboFect, incubated for 20 min, and added to the cells.

BIAcore Experiments—Experiments were conducted on a BIAcore T200 instrument (GE Healthcare). Ran was immobilized on a CM5 sensor chip by amine coupling as described by the manufacturer using 20 μg/ml Ran in 10 mM NaOAc, pH 5.0, and 2 mM $MgCl_2$. Typically, this resulted in immobilization of ~2000 response units of Ran on the sensor chip surface. All experiments were performed in transport buffer containing 20 mM Hepes/KOH, pH 7.3, 110 mM potassium acetate, 2 mM magnesium acetate, 1 mM EGTA, and 2 mM DTT at a flow rate of 10 ml/min at 25 °C. The Ran surface was regenerated by injecting 60 s with a flow rate of 30 μl/min of 1 M $MgCl_2$ for MycBP2 or 0.01% SDS for RCC1. Single cycle kinetics were measured with five different concentrations of RCC1 or MycBP2 (1–25 nM).

Single Cycle GTPase Assay—The assay was performed as described previously (36, 37). Briefly, purified Ran (2 μM) was loaded with [γ-^{32}P]GTP (6000 Ci/mmol) in the presence of 10 mM EDTA, 2 mM DTT, and 20 μM GTP. GTP was taken from a stock containing 200 μM GTP, 20 mM Hepes/KOH, pH 7.3, and 20 mM $MgCl_2$. After 30 min of incubation at room temperature, $MgCl_2$ was adjusted to a final concentration of 20 mM, and the sample was diluted with an equal volume of transport buffer. Then loaded Ran (2 μM) was incubated for 10 min at room temperature in 40 μl of GAP Assay buffer (36 mM Tris/HCl, pH 8.0, 75 mM NaCl, 6 mM $MgCl_2$, 1 mM DTT) with 0.4 mM GTP in presence of RanGAP1 (100 nM) or MYCBP2 (35 nM) or both. The reaction was stopped by addition of 1 ml of cold Stopping buffer (5% activated charcoal in NaH_2PO_4). The mixture was centrifuged (5 min, room temperature, 8000 × *g*), and the [^{32}P]P_i in the supernatant was determined as described previously (25).

Mant-GDP-release Assay—The assay was performed as described previously (36). To exchange the Ran-bound GDP with the fluorescently labeled mant-GDP, Ran (100 μM) was incubated for 2 h at room temperature in the presence of 500 μM mant-GDP in 20 mM Hepes, pH 7.3, 10 mM EDTA, 2 mM $MgCl_2$, 110 mM potassium acetate, and 2 mM DTT. Unbound nucleotide was removed by gel filtration over a Sephadex G-25 column (GE Healthcare) in transport buffer. The concentration of the nucleotide-loaded Ran was measured by Bradford. For the analysis of the Ran/GEF interaction, Ran-mant-GDP (2 μM) was incubated in the presence of 35 nM RCC1 or MycBP2 and 200 μM GDP at 25 °C in 50 mM Tris/HCl, pH 7.4, 5 mM $MgCl_2$, 5 mM DTT. The reaction rates of the GEF-catalyzed GDP dissociation on Ran were measured as a decrease in fluorescence (excitation 366 nm; emission 450 nm) due to energy transfer, using an EnSpire multimode plate reader fluorescence spectrophotometer.

GTP Binding Assay—[^{35}S]GTPγS binding assay was performed with some modifications as described previously (25,

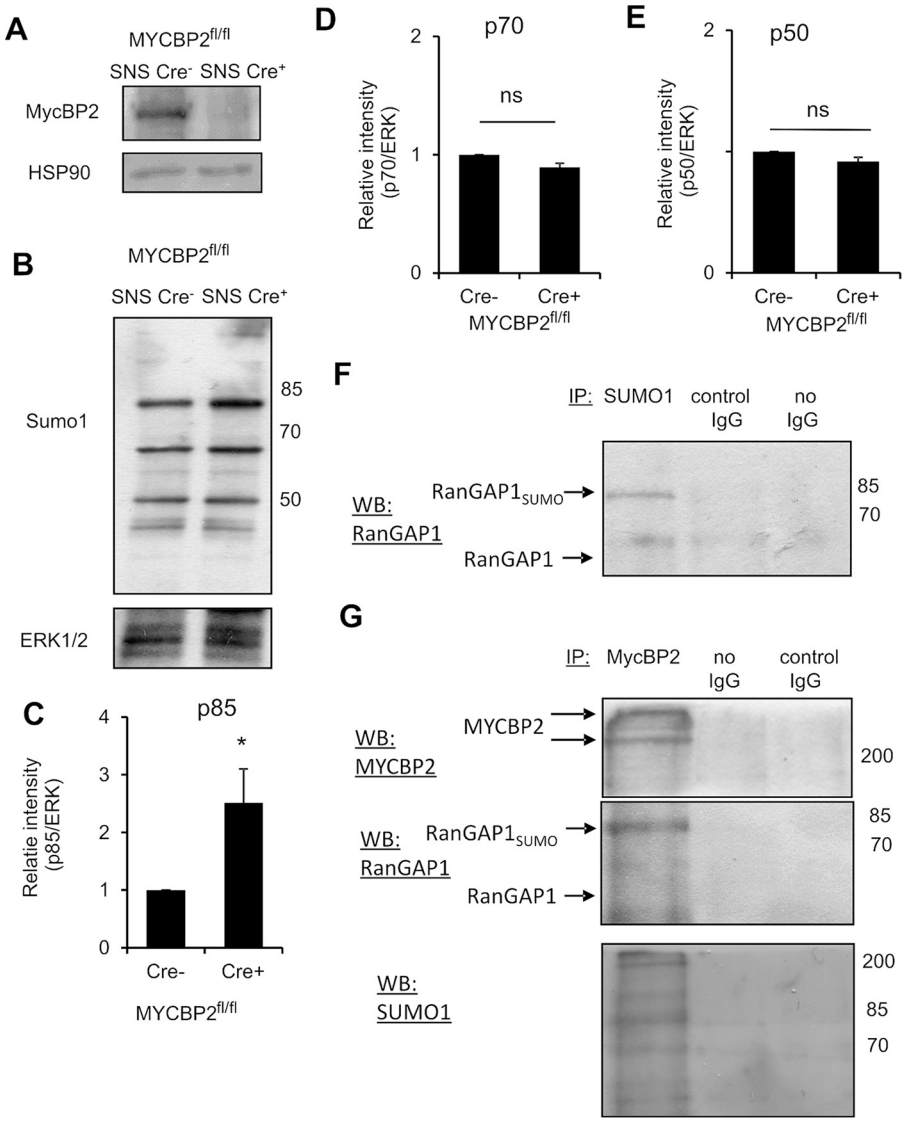

FIGURE 1. **SUMOylated RanGAP1 physically interacts with MYCBP2.** *A,* representative Western blot (*WB*) with antibodies against MYCBP2 of DRG lysates from naive SNS Cre^- $MYCBP2^{fl/fl}$ mice is shown. Equal loading was confirmed using HSP90 expression. *B,* representative Western blot with antibodies against SUMO1 of DRG lysates from naive SNS Cre^- and Cre^+ $MYCBP2^{fl/fl}$ mice is shown. Equal loading was confirmed using ERK1/2 expression. *C–E,* densitometric analyses of the three major protein bands with a size of 85 kDa (*C*), 70 kDa (*D*), and 50 kDa (*E*). *ns*, not significant. Data are shown as mean ± S.E. ($n = 3–5$). Two-tailed Student's *t* test, *, $p < 0.05$. *F,* immunoprecipitation (*IP*) of RanGAP1 from DRG lysates of wild type mice using an antibody against SUMO1, an independent antibody (*control IgG*), or no antibody (*no IgG*). SUMOylated RanGAP1 was detected using an antibody against RanGAP1. *G,* immunoprecipitation of DRG lysate from wild type mice using an antibody against MYCBP2, an independent antibody (*control IgG*), or no antibody (*no IgG*). The immunoprecipitations were analyzed using antibodies against MYCBP2 or RanGAP1 or SUMO1. The position of the two major MYCBP2 splice variants and of RanGAP1 and SUMOylated RanGAP1 is indicated by *arrows*.

38). Briefly, Ran (2 μM) was incubated at room temperature with 15 μM GDP and 1 nM [^{35}S]GTPγS (1250 Ci/mmol) (PerkinElmer Life Sciences) in the absence or presence of RanGAP1 (100 nM), MYCBP2 (0–50 nM), or both. RCC1 (35 nM) was used as control. The assay was performed in 250 μl of binding buffer (50 mM Tris/HCl, pH 7.4, 3 mM $MgCl_2$, 100 nM NaCl, 200 μM EDTA, 1 mM DTT) for 30 min. The samples were filtered through nitrocellulose filters (Millipore, Ma), washed six times with 250 μl of binding buffer, dried, and analyzed by liquid scintillation counting. MYCBP2 alone was used as control to correct for unspecific binding of [γ-^{35}S]GTP.

Real Time RT-PCR—The assay was performed as described previously (39). 24 h after zymosan injection, Ran mRNA was measured in DRGs by real time RT-PCR, with the 5′ and 3′ primers GTATTGTGTGGCAACAAAAGTG and GAGCTTTCTGGCAAGCCAG, respectively. A 153-bp product was detected with the following amplification program: 95 °C for 15 min, 1 cycle; 94 °C for 15 s, 55 °C for 30 s, and 72 °C for 30 s, 40 cycles. GAPDH mRNA levels of the samples were measured as internal controls; the 5′ and 3′ primers were CAATGTGTCCGTCGTGGATCT and GTCCTCAGTGTAGCCCAAGATG, respectively, with the same amplification program as for Ran mRNA. PCR was conducted in triplicate, and the ratios of Ran *versus* GAPDH signals represent the normalized levels of Ran expression.

Statistics—Experiments with only two treatment groups were analyzed for statistical significance using Student's *t* test. Experiments with more than two groups were analyzed using

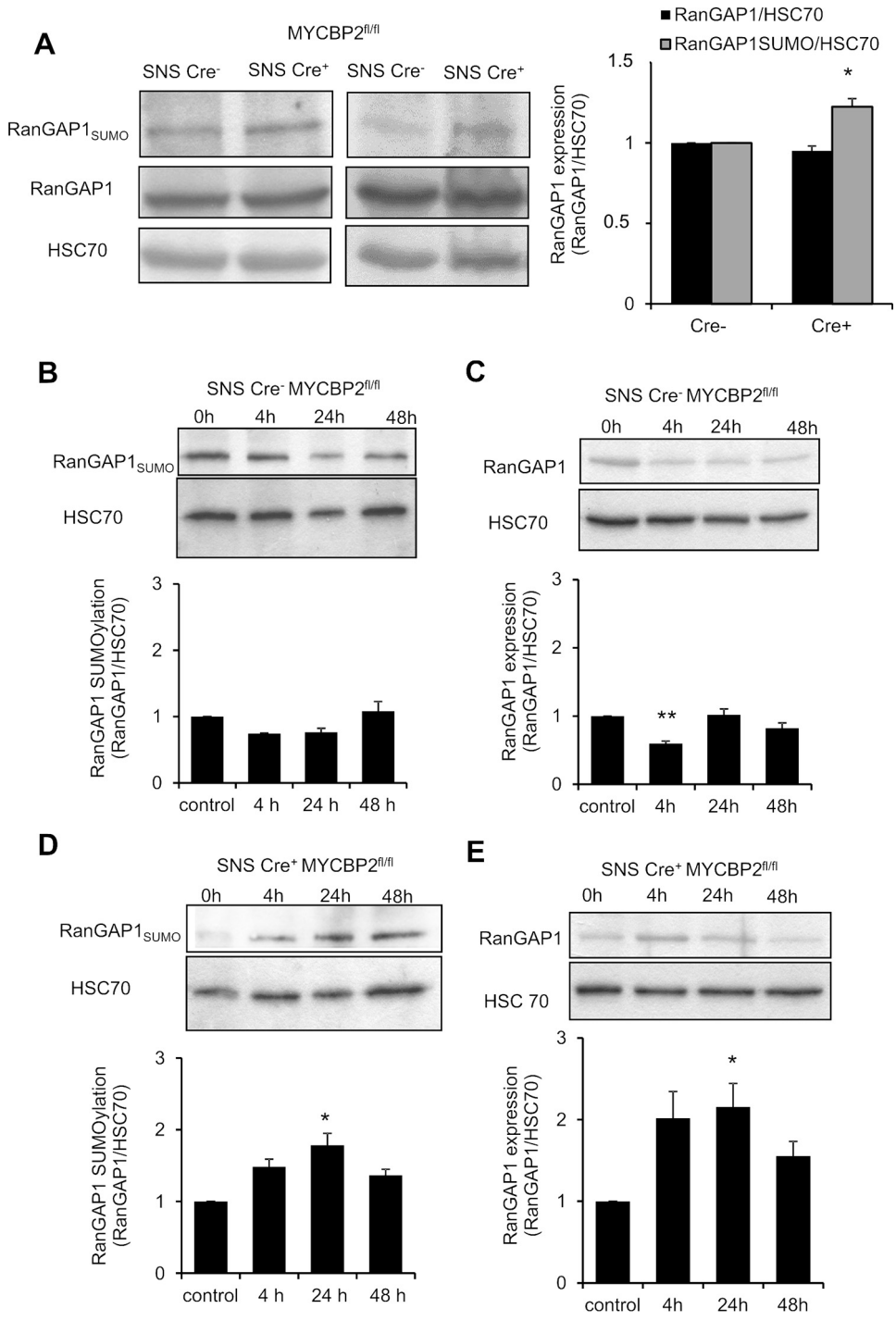

FIGURE 2. **During inflammatory hyperalgesia MYCBP2 deficiency induces the up-regulation of RanGAP1 expression in DRGs.** *A,* expression of RanGAP1 and SUMOylated RanGAP1 in DRGs from SNS-Cre$^-$ and Cre$^+$ MYCBP2$^{fl/fl}$ mice. Equal loading was confirmed using HCS70 expression. The *right panel* shows the densitometric analysis. Data are shown as mean ± S.E. ($n = 3$). Two-tailed Student's *t* test; *, $p < 0.05$. *B–E,* expression of SUMOylated RanGAP1 (*B* and *D*) and unmodified RanGAP1 (*C* and *E*) in DRGs from SNS-Cre$^-$ (*B* and *C*) and Cre$^+$ (*E* and *D*) MYCBP2$^{fl/fl}$ mice. Expression was tested in naive mice 4, 24, and 48 h after zymosan injection in one hind paw (20 μl, 12.5 mg/ml).

one- or two-way analysis of variance (ANOVA) with Dunnett's post hoc test. Significance was accepted at $p < 0.05$.

Results

SUMOylated RanGAP1 Physically Interacts with MYCBP2 and Mediates Its Translocation to the Nucleus—Previously, we studied the effect of a selective MYCBP2 deletion in nociceptive and thermoreceptive neurons of the DRGs (Fig. 1*A*) on protein expression in DRG neurons using an antibody microarray covering 750 proteins (20). The array showed the up-regulation of SUMO1 and/or SUMOylated proteins in MYCBP2-deficient DRGs. In these mice, Cre expression was under control of the Nav1.8 (SNS) promotor. We verified this finding using Western blot analysis with DRGs from SNS Cre-positive and -negative

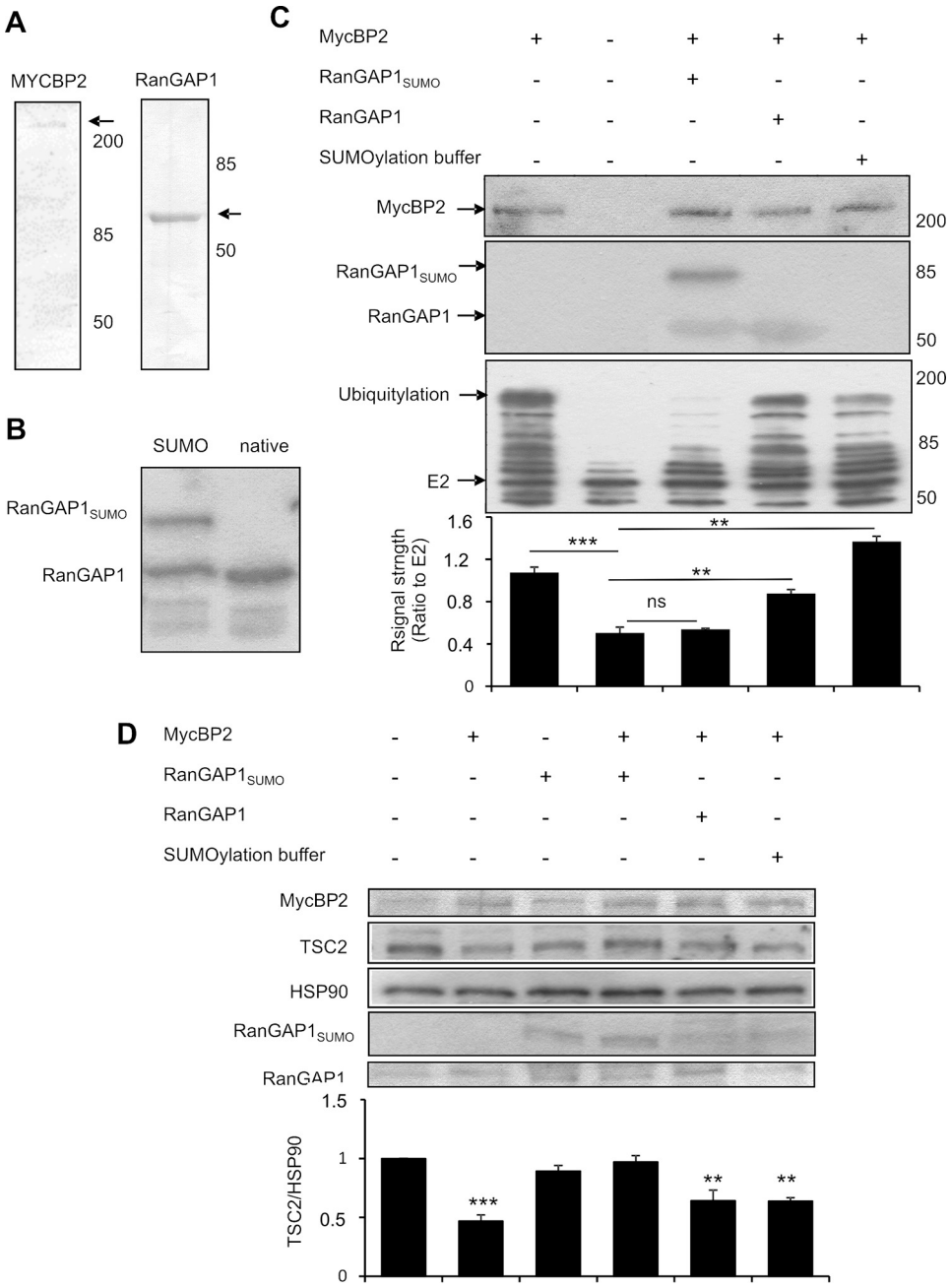

FIGURE 3. **SUMOylated RanGAP1 inhibits the ubiquitin ligase activity of MYCBP2.** *A,* Coomassie-stained gels of purified MYCBP2 and RanGAP1. 50 ng of protein was analyzed using 10% SDS-PAGE. *B,* representative Western blot for RanGAP1 SUMOylation using RanGAP1 antibody (GTX62316). 60–70% of RanGAP1 is SUMOylated in every SUMOylation assay. *C, in vitro* ubiquitylation assay for MYCBP2 using His-tagged ubiquitin in the absence or presence of SUMOylated RanGAP1, unmodified RanGAP1, or SUMOylation buffer. The samples were analyzed by Western blot for MycBP2, RanGAP1, or His-tagged ubiquitin. The *lower panel* shows the densitometric analysis of signals seen with the antibodies against His and are corrected for loading by normalization for the His-tagged E2 protein. Data are shown as mean ± S.E. ($n = 3$). One-way ANOVA/Dunnett's test, **, $p < 0.01$; ***, $p < 0.001$; *ns*, not significant. *D, in vitro* assay to study degradation of TSC2 in HeLa lysates in the absence or presence of SUMOylated RanGAP1, unmodified RanGAP1, or SUMOylation buffer. TSC2 levels were determined by Western blot analysis. Equal loading was confirmed using HSP90 expression. The *lower panel* shows the densitometric analysis of three independent experiments. Data are shown as mean ± S.E. One-way ANOVA/Dunnett's test. **, $p < 0.01$; ***, $p < 0.001$.

$MYCBP2^{fl/fl}$ mice revealing a significant up-regulation of a protein of ~85 kDa in the absence of MYCBP2 (Fig. 1, *B* and *C*). The expression of two other major bands (50 and 70 kDa) recognized by the antibody against SUMO1 was not altered in MYCBP2-deficient DRGs (Fig. 1, *D* and *E*). RanGAP1 is well known to be modified by SUMO1 binding and has after SUMOylation a molecular mass of ~85 kDa (40). To test whether or not SUMOylated RanGAP1 is present in DRGs, we immunoprecipitated proteins from DRGs with an antibody against SUMO1 and detected SUMOylated RanGAP1 in the precipitate using an antibody against RanGAP1 (Fig. 1*F*). To test for a physical interaction of MYCBP2 with RanGAP1, we immunoprecipitated MYCBP2 from DRGs of wild type mice and found that SUMOylated RanGAP1 co-immunoprecipitated with MYCBP2, although the unmodified form of RanGAP1 was not detected in the immunoprecipitate (Fig. 1*G*).

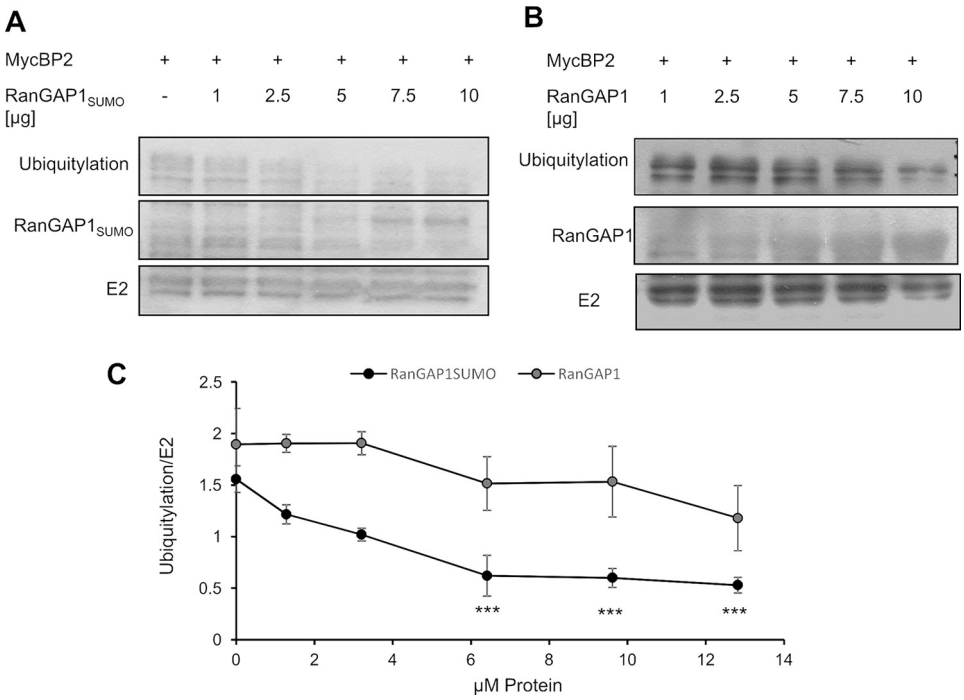

FIGURE 4. **SUMOylated RanGAP1 inhibits the ubiquitin ligase activity of MYCBP2.** *A* and *B, in vitro* ubiquitylation assay for MYCBP2 using His-tagged ubiquitin in the presence of different concentrations of SUMOylated RanGAP1 (1–10 μg; *A*) or unmodified RanGAP1 (1–10 μg, *B*). The samples were analyzed by Western blot for RanGAP1 or His-tagged ubiquitin. *C,* densitometric analysis of signals seen with the antibodies against His and corrected for loading by normalization for the His-tagged E2 protein. Data are shown as mean ± S.E. ($n = 3$). One-way ANOVA/Dunnett's test, ***, $p < 0.001$.

Next, we determined RanGAP1 expression in DRGs in the presence and absence of MYCBP2. Using a RanGAP1 antibody, we found a small but significant up-regulation of the SUMOylated form of RanGAP1 in MYCBP2-deficient DRGs, whereas expression of the unmodified form of RanGAP1 was not altered (Fig. 2*A*). MYCBP2 has been previously shown to mediate inflammatory hyperalgesia by altering neuronal functions in DRGs and spinal cords (12, 20). Therefore, we determined RanGAP1 expression in DRGs from SNS Cre-negative $MYCBP2^{fl/fl}$ mice during zymosan-induced hyperalgesia. The level of SUMOylated RanGAP1 in DRGs was not altered by the inflammation (Fig. 2*B*), and the expression of nonmodified RanGAP1 showed only a small decrease 4 h after zymosan injection (Fig. 2*C*). More importantly, in the absence of MYCBP2, a significant up-regulation of SUMOylated (Fig. 2*D*) and nonmodified RanGAP1 (Fig. 2*E*) was seen 24 h after zymosan injection in the DRGs.

SUMOylated RanGAP1 Inhibits MYCBP2 Activity and Mediates Its Transport to the Nucleus—Because MYCBP2 is an E3 ubiquitin ligase, we determined whether or not MYCBP2 regulates expression levels of SUMOylated RanGAP1 by targeting it for degradation through polyubiquitylation. Therefore, we tested the ability of purified human MYCBP2 (Fig. 3*A*) (20, 28) to ubiquitylate purified recombinant human RanGAP1 in its unmodified and its SUMOylated form (8, 32). The SUMOylation reaction yielded around 65% of SUMOylated RanGAP1 (Fig. 3*B*). Surprisingly, we did not find MYCBP2-dependent ubiquitylation of SUMOylated RanGAP1 but instead a strong inhibition of the ubiquitin ligase activity of MYCBP2 in the presence of SUMOylated RanGAP1, as determined by the presence of ubiquitylated proteins (Fig. 3*C*). This effect was specific for SUMOylated RanGAP1, because the unmodified form of RanGAP1 did not affect MYCBP2-dependent protein ubiquitylation (Fig. 3*C*). To validate the inhibitory effect of SUMOylated RanGAP1 on the ubiquitin ligase activity of MYCBP2, we tested the influence of SUMOylated RanGAP1 on the ubiquitin-mediated MYCBP2-dependent degradation of its known target TSC2 (17, 21, 25). Fittingly, SUMOylated RanGAP1 prevented MYCBP2-dependent degradation of TSC2 (Fig. 3*D*), although the unmodified form of RanGAP1 had again no effect on MYCBP2-dependent ubiquitylation of TSC2 (Fig. 3*D*). The effect of SUMOylated RanGAP1 on MYCBP2 autoubiquitylation was concentration-dependent, although the unmodified form of RanGAP1 had no significant effect on MYCBP2 activity (Fig. 4, *A* and *B*). SUMOylated RanGAP1 inhibited MYCBP2 activity with an IC_{50} of ~4 μM (Fig. 4*C*).

SUMOylation of RanGAP1 after cellular stimulation (*i.e.* serum stimulation) is known to cause its translocation to the nuclear pore complex where it acts as GAP for Ran (8, 9, 44). Both proteins, RanGAP1 and MYCBP2, are expressed in DRG neurons, as shown by co-staining with the neuronal marker NeuN (Fig. 5*A*), and incubation with 10% FBS stimulated RanGAP1 SUMOylation (Fig. 5*B*) without altering MYCBP2 expression (Fig. 5*C*). Interestingly, serum stimulation increased the number of DRG neurons showing nuclear localization of RanGAP1 (Fig. 5*D*). Similarly, the number of DRG neurons showing nuclear MYCBP2 localization increased (Fig. 5*E*). Notably, the cytoplasmic expression of tubulin was not affected by the serum treatment showing the specificity of the change in localization for RanGAP1 and MYCBP2 (Fig. 5*F*).

To study whether or not SUMOylated RanGAP1 mediates MYCBP2 translocation to the nucleus, we transfected DRG

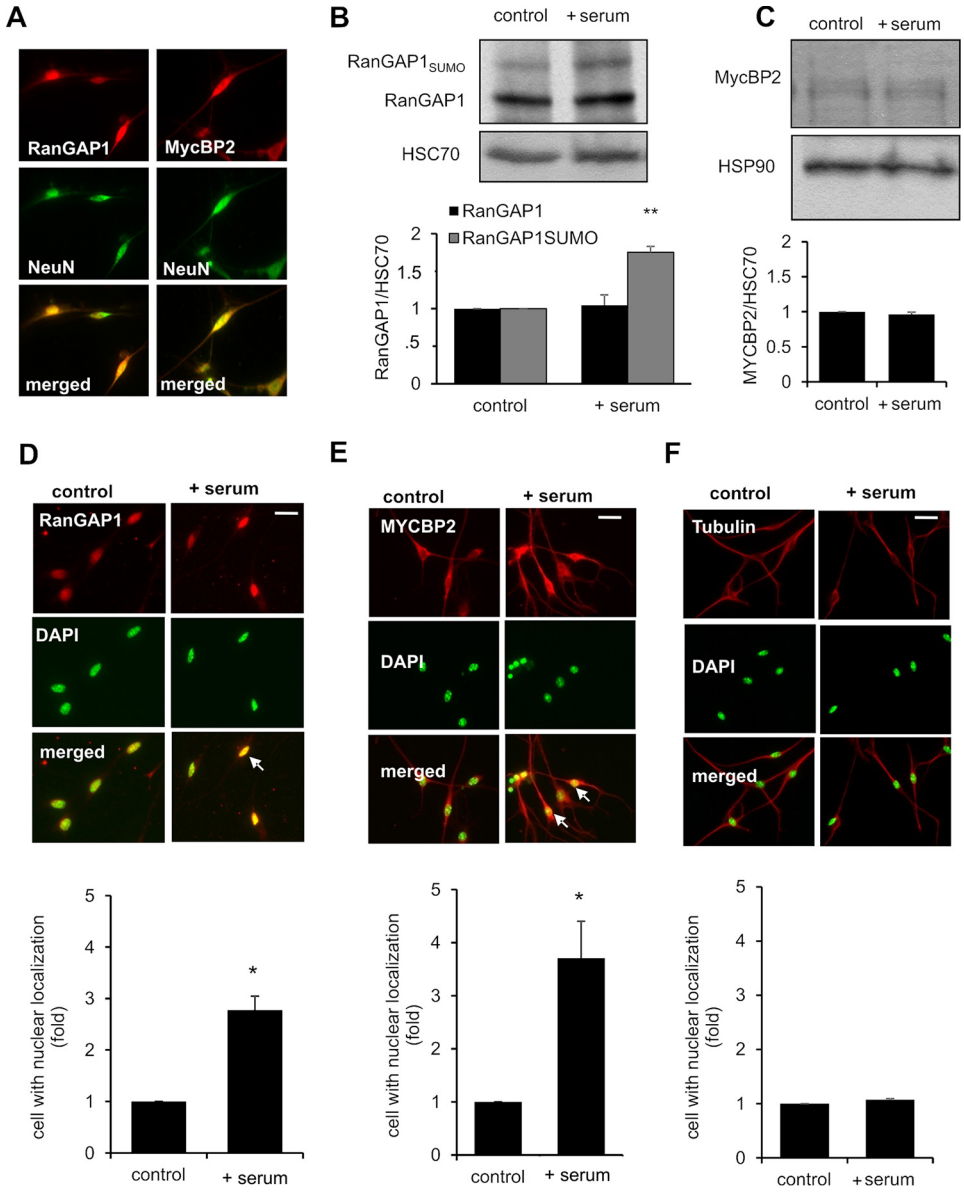

FIGURE 5. **RanGAP1 and MYCBP2 localization at the nucleus of DRG neurons is increased after serum stimulation.** *A,* representative images of RanGAP1 and MycBP2 expression (*red*) in primary neuron cultures of DRGs. Neurons were identified by NeuN staining (*green*). *B,* RanGAP1 expression in primary cultures of DRGs after 10% FBS stimulation for 3 h. The samples were analyzed by Western blot for RanGAP1. Equal loading was confirmed using HSC70 expression. The *lower panel* shows the densitometric analysis. Data are shown as mean ± S.E. ($n = 3$). Student's *t* test, **, $p < 0.01$. *C,* MycBP2 expression in primary cultures of DRGs after 10% FBS stimulation for 3 h. The samples were analyzed by Western blot for MycBP2. Equal loading was confirmed using HSP90 expression. The *lower panel* shows the densitometric analysis. Data are shown as mean ± S.E. ($n = 3$). *D,* representative images of RanGAP1 localization (*red*) in primary neuron cultures of DRGs in regard to nuclei (DAPI, *green*). RanGAP1 localization was determined in untreated primary cultures of DRG neurons from wild type mice or after 3 h of stimulation with 10% FBS. The *white bar* represents 20 μm. *Arrows* depict cells showing nuclear RanGAP1 localization. In the *lower panel* the determination of nuclear localization using densitometric line profiles (ImageJ 1.43) is shown. Data are shown as mean ± S.E. ($n = 50$). Two-tailed Student's *t* test, *, $p < 0.05$. *E,* representative images of MYCBP2 localization (*red*) in primary neuron cultures of DRGs in regard to nuclei (DAPI, *green*). MYCBP2 localization was determined in untreated primary cultures of DRG neurons from wild type mice or after 3 h stimulation with 10% FBS. *Arrows* depict cells showing nuclear MYCBP2 localization. The *white bar* represents 20 μm. In the *lower panel* the determination of nuclear localization using densitometric line profiles (ImageJ version 1.43) is shown. Data are shown as mean ± S.E. ($n = 50$). Two-tailed Student's *t* test, *, $p < 0.05$. *F,* representative images of β-tubulin localization (*red*) in primary neuron cultures of DRGs in regard to nuclei (DAPI, *green*). β-Tubulin localization was determined in untreated primary cultures of DRG neurons from wild type mice or after 3 h stimulation with 10% FBS. The *white bar* represents 20 μm. In the *lower panel* the determination of nuclear localization using densitometric line profiles (ImageJ version 1.43). Data are shown as mean ± S.E. ($n = 50$).

neurons with siRNA against RanGAP1 and identified the transfected neurons using FITC-labeled siRNA. Transfection of siRNA against RanGAP1 caused significant down-regulation of RanGAP1 in the DRG neurons (Fig. 6*A*). Next, DRG neurons were transfected with RanGAP1 siRNA or nontargeting control siRNA and stimulated with 10% FBS. The transfected neurons showed a significant decrease in the number of cells with nuclear localization of MYCBP2 in the absence of RanGAP1, which was reconstituted after overexpression of human RanGAP1 (Fig. 6, *B* and *C*).

To test whether or not the RanGAP1-dependent translocation of MYCBP2 was also seen in other cells, we studied the translocation of RanGAP1 and MYCBP2 in serum-stimulated HeLa cells, which express both proteins endogenously. Indeed,

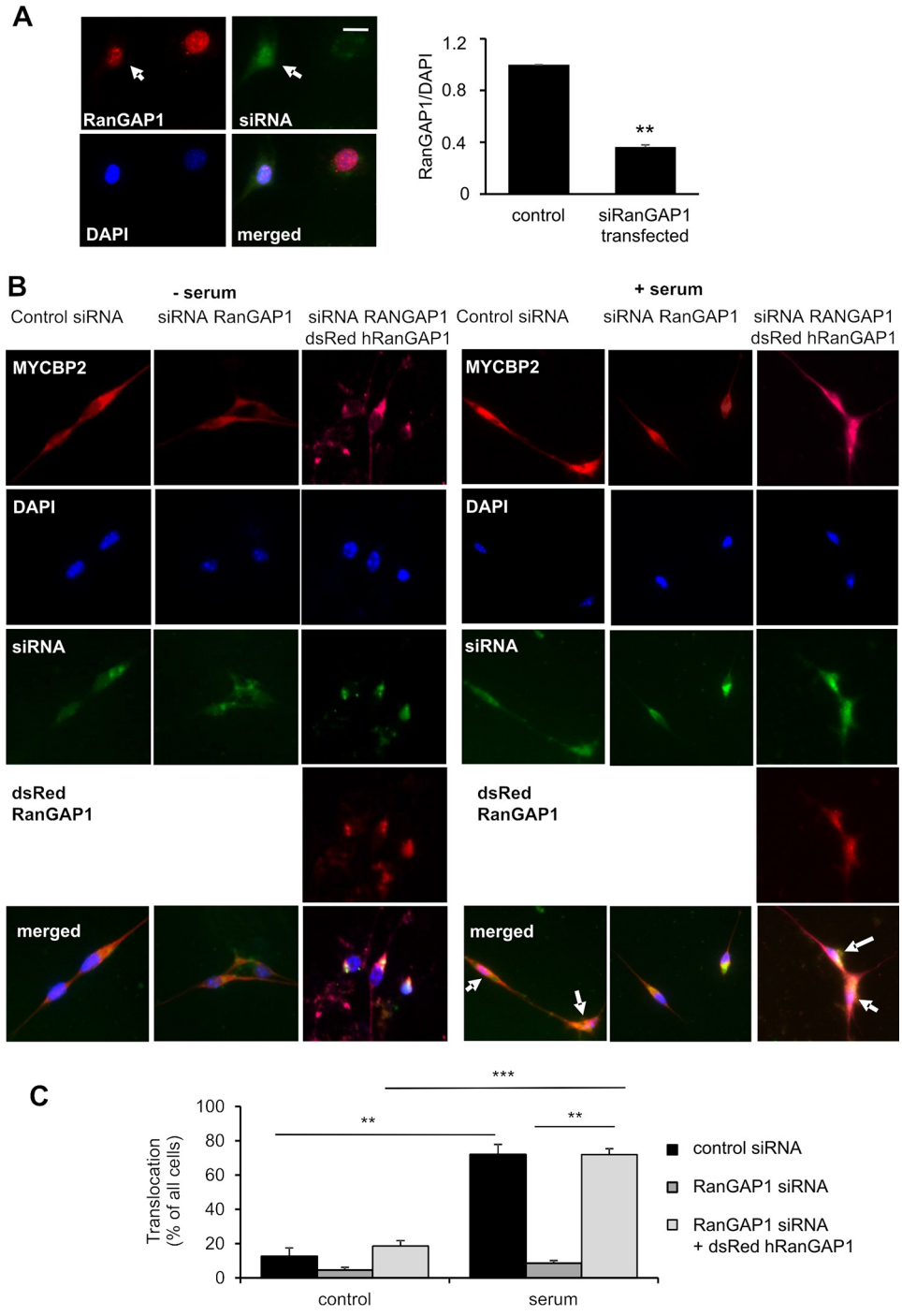

FIGURE 6. **Serum-induced nuclear localization of MYCBP2 is mediated by RanGAP1.** *A,* representative images of RanGAP1 expression in primary DRG cultures 48 h after transfection with siRNA against RanGAP1 or nontarget siRNA. *Arrows* depict a transfected cell. The *right panel* shows the densitometric analysis of RanGAP1 expression in primary DRG cultures 48 h after transfection with siRNA. Data are shown as mean ± S.E. ($n = 3$). Student's *t* test, **, $p < 0.01$. *B* and *C,* representative images (*B*) and quantification of nuclear localization (*C*) of MYCBP2 in primary neurons. MYCBP2 (Cy3-labeled (*red*) or Cy5-labeled (*pink*)), nuclei (DAPI, *blue*), FITC-labeled-siRNA (*green*), and human DsRed-coupled human RCC1 (*red*) are shown. MYCBP2 localization was determined in transfected primary DRG neurons 48 h after transfection with siRNA against RanGAP1, nontarget siRNA, or RanGAP1 together with human dsRed-RanGAP1 (rescue). Cells were untreated (− serum) or stimulated for 3 h with 10% serum. *White arrows* indicate cells with nuclear MYCBP2 localization. The *white bar* represents 10 μm. Data are shown as mean ± S.E. ($n = 50$ cells). One-way ANOVA/Dunnett's test, **, $p < 0.01$; ***, $p < 0.001$.

immunocytochemical analysis showed a serum-induced translocation of both proteins (Fig. 7, *A* and *B*), Accordingly, the MYCBP2 protein amount increased in nuclear extracts of these cells (Fig. 7*C*). Likewise, the amount of SUMOylated RanGAP1 was significantly increased in serum-treated cells (Fig. 7*D*). Again, down-regulation of RanGAP1 by siRNA prevented the serum-induced translocation of MYCBP2 (Fig. 7, *E* and *F*). Thus, the data demonstrate that RanGAP1 is necessary for the transport of MYCBP2 to the nucleus.

MYCBP2 Is a Nuclear GEF for Ran in DRG Neurons—Next, we studied whether or not MYCBP2 modulates the interaction between Ran/RanGAP1. First, we performed a single cycle

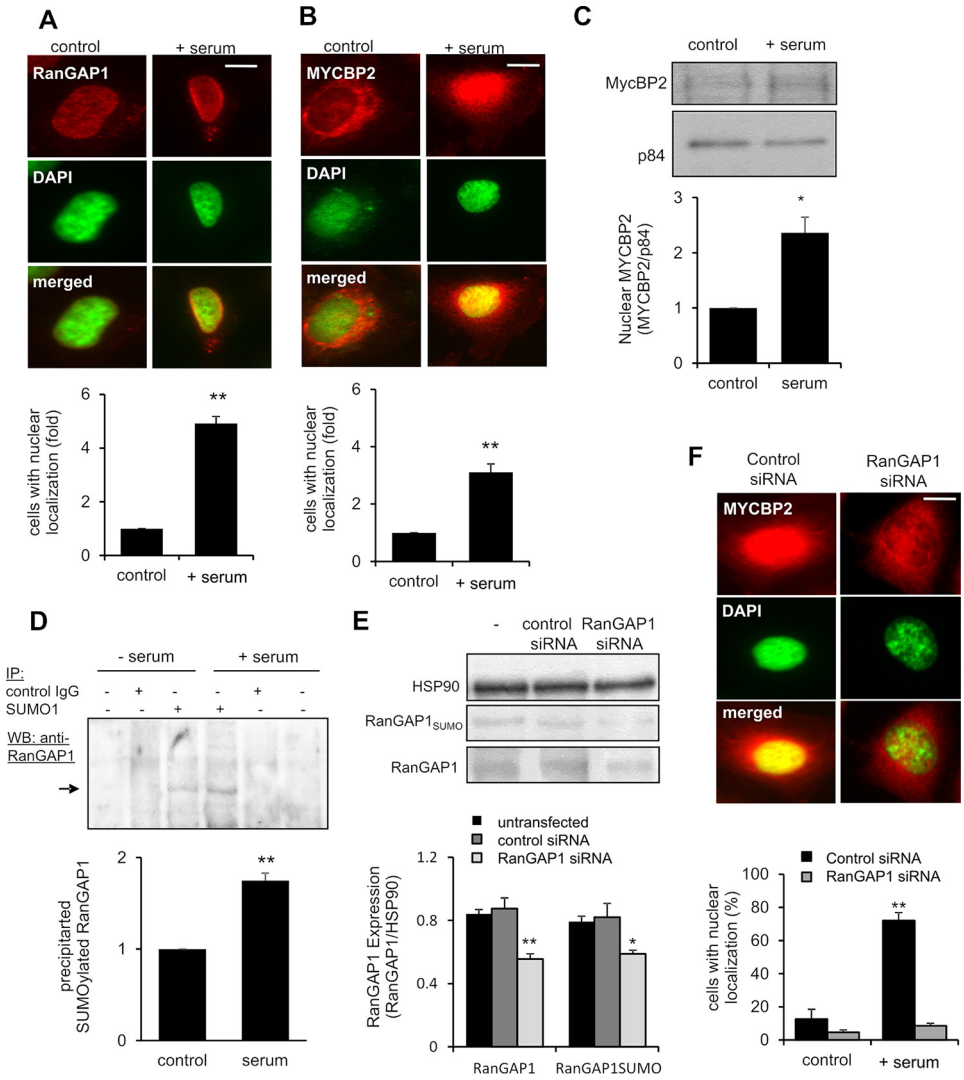

FIGURE 7. **RanGAP1 and MYCBP2 localization at the nucleus of HeLa cells is increased after serum stimulation.** *A,* representative images of RanGAP1 localization (*red*) in HeLa cells in regard to nuclei (DAPI, *green*). RanGAP1 localization was determined in untreated HeLa cells or after 0.5 h of stimulation with 10% FBS. The *white bar* represents 20 μm. *Lower panel,* determination of nuclear localization using densitometric line profiles. Data are shown as mean ± S.E. ($n = 50$). Two-tailed Student's *t* test, **, $p < 0.01$. *B,* same as *A* except that MYCBP2 localization is shown. Data are shown as mean ± S.E. ($n = 50$). Two-tailed Student's *t* test, **, $p < 0.05$. *C,* MycBP2 expression in HeLa nuclei after 10% FBS stimulation for 0.5 h. The samples were analyzed by Western blot for MycBP2 and the nuclear matrix protein p84 as loading control. Equal loading was confirmed using p84 expression. *Lower panel,* densitometric analysis. Data are shown as mean ± S.E. ($n = 3$). Student's *t* test, *, $p < 0.05$. *D,* immunoprecipitation (*IP*) without antibody, with control IgG or with antibodies against SUMO1 with or without serum stimulation (10% FBS; 3 h). Western blot (*WB*) analysis was performed using antibodies against RanGAP1. *Lower panel* shows the densitometric analysis of the immunoprecipitated SUMOylated RanGAP1 with or without serum treatment. Data are shown as mean ± S.E. ($n = 3$). One-way ANOVA/Dunnett's test, **, $p < 0.01$. *E,* determination of SUMOylated RanGAP1 and RANGAP1 expression after siRNA transfection. The samples were analyzed by Western blot for RanGAP1. *Lower panel,* densitometric analysis. Data are shown as mean ± S.E. ($n = 3$). Two-tailed Student's *t* test, *, $p < 0.05$; **, $p < 0.01$. *F,* representative images and quantification of nuclear localization of MYCBP2 in HeLa cells. MYCBP2 (*red*) and nuclei (DAPI, *green*) are shown. MYCBP2 localization was determined in HeLa cells 48 h after transfection with siRNA against RanGAP1 or nontarget siRNA. Cells were stimulated for 0.5 h with 10% serum. The *white bar* represents 10 μm. Data are shown as mean ± S.E. ($n = 50$ cells). One-way ANOVA/Dunnett's test, **, $p < 0.01$.

GTPase assay to investigate whether MYCBP2 increases the GAP activity of RanGAP1 toward purified Ran (Fig. 8*A*), and we found that MycBP2 was a weak inhibitor of the GAP activity of RanGAP1 (Fig. 8*B*). Thus, RanGAP1 and MYCBP2 either compete for Ran binding or MYCBP2 reduces RanGAP1 activity through stabilization of GTP-bound Ran. However, MYCBP2 contains an N-terminal RCC1-like domain (Fig. 8*C*) (13), and RCC1 is a known GEF for Ran, indicating a potential functional interaction between MYCBP2 and Ran. Indeed, when the binding affinities of purified MYCBP2 and RCC1 to immobilized Ran were tested using a BIAcore T200, we found similar binding affinities for both proteins (MYCBP2, K_D 1.14 nM; RCC1, K_D 2.95 M) (Fig. 8*D*). To test whether or not MYCBP2 acts as a GEF for Ran, we studied the release of mant-GDP from Ran in the presence of its known GEF RCC1 or MYCBP2. Both RCC1 and MYCBP2 induced the mant-GDP release with similar half-times (80 ± 15 and 67 ± 14 s, respectively) (Fig. 8*E*).

Also, the GTP binding was tested with [^{35}S]GTPγS binding assays in the presence or absence of RCC1, MYCBP2, and RanGAP1. As expected, the presence of RanGAP1 alone had only a negligible effect on [^{35}S]GTPγS binding of Ran. In contrast, MYCBP2 significantly increased the amount of [^{35}S]GTPγS bound to Ran, which was further enhanced in the presence of both MYCBP2 and RanGAP1 (Fig. 9*A*). This synergistic effect

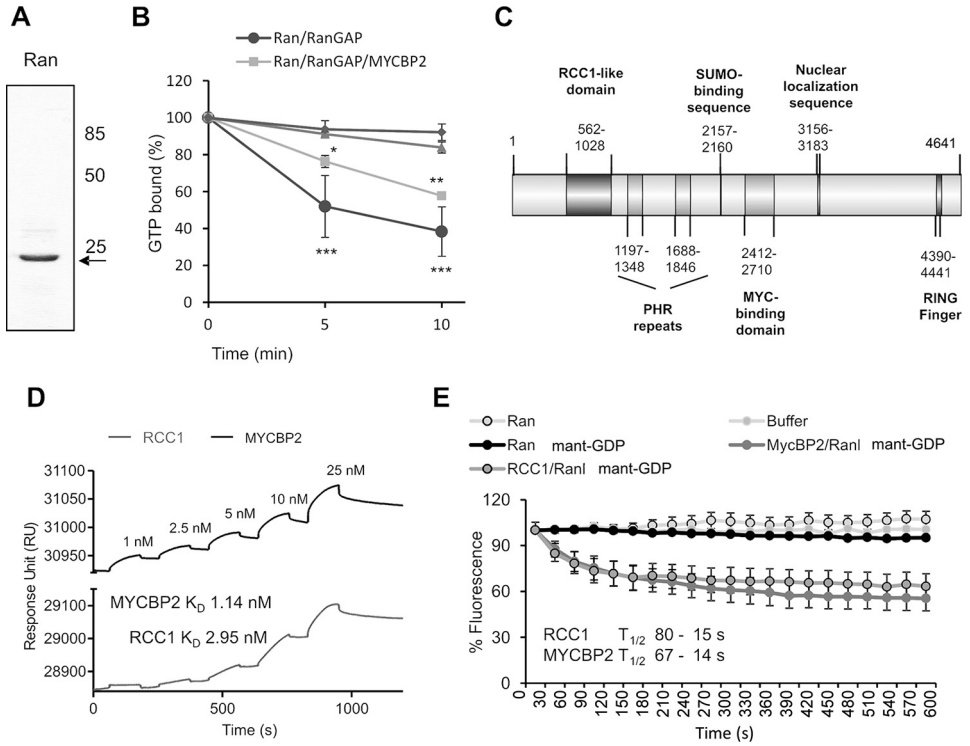

FIGURE 8. **MYCBP2 is interacting with Ran.** *A,* Coomassie-stained gel of purified Ran. 50 ng of protein was analyzed using 12% SDS-PAGE. *B*, single cycle GTPase activity of Ran (2 nM) with or without RanGAP1 (100 nM) and/or MYCBP2 (25 nM) after 0, 5, and 10 min. Data are presented as mean ± S.E. ($n = 3$). Two-way ANOVA/Bonferroni test, *, $p < 0.05$; **, $p < 0.01$; ***, $p < 0.001$. *C,* scheme depicting the protein domains of MYCBP2. The *numbers* refer to the amino acid sequence of full-length human MYCBP2. *D,* representative data of BIAcore single cycle kinetics with immobilized Ran and different RCC1 or MYCBP2 concentrations (1–25 nM) and determined K_D values for the interaction of RanGDP with RCC1 (2.95 nM) or MYCBP2 (1.14 nM). *E,* mant-GDP release assay to determine GDP release factor activity of MycBP2 (35 nM) in the presence of 2 μM mant-GDP loaded Ran. RCC1 (35 nM) was used as positive control. Data are presented as mean ± S.E. ($n = 3$).

either shows activation of the GEF activity of MYCBP2 or is due to the fact that RanGAP1 stimulates GTP hydrolysis of Ran and therefore increases the availability of GDP-bound Ran for MYCBP2. However, stimulation of [^{35}S]GTPγS binding by MYCBP2 alone was around 70% of the [^{35}S]GTPγS binding induced by equimolar amounts of RCC1 (Fig. 9*A*). MYCBP2-induced increase of [^{35}S]GTPγS binding by Ran was concentration-dependent (Fig. 9*B*), and the recombinant RCC1-like domain of MYCBP2 was sufficient to increase [^{35}S]GTPγS binding of Ran (Fig. 9*C*), suggesting that this domain carries the GEF activity of MYCBP2. Substitution of His-2912 and His-913 in the RCC1-like domain of MYCBP2 by alanine has been shown to diminish its inhibitory activity for adenylyl cyclases. Accordingly, insertion of the double mutation in the RCC1-like domain abolished the GEF activity toward Ran (Fig. 9*C*). Fittingly, the Myc-binding domain of MYCBP2 that is sufficient to allow binding to Myc and actin, but lacks the RCC1-like domain, was not sufficient to increase GTP binding of Ran (Fig. 9*C*). Next, we tested whether or not inactive (T24N) or constitutively active (Q69L) Ran is able to block the interaction between Ran and MYCBP2. Both mutants were preloaded with GTP or GDP, and free nucleotides were removed before the assay. We found that only the inactive Ran mutant interfered with the GEF activity of MYCBP2 for Ran (Fig. 9*D*). Fittingly, MYCBP2 co-precipitated only with the T24N mutant in pull-down experiments employing wild type, Q69L, and T24N Ran (Fig. 9*E*) supporting a higher affinity of MYCBP2 for GDP-bound Ran than for GTP-bound Ran.

In the next step, we investigated whether or not MYCBP2 deficiency alters the localization of Ran in DRG neurons. First, we used immunohistochemistry of DRGs of wild type mice and found that MYCBP2 co-localized in part with Ran at the nucleus (Fig. 10, *A* and *B*). Comparison of the Ran localization in nuclei of DRGs from SNS Cre-negative and Cre-positive MYCBP2$^{fl/fl}$ mice showed that in the absence of MYCBP2 the ratio of cytosolic and nuclear Ran is shifted toward a nuclear localization of Ran (Fig. 10, *C* and *D*), suggesting that the GEF activity of MYCBP2 is necessary to induce the nuclear export of GTP-bound Ran. To investigate whether or not loss of MYCBP2 interferes with the localization of Ran cargo proteins, we determined the localization of NFκB in isolated nuclei of DRGs from mice during zymosan-induced peripheral inflammation. We found that 3 h after zymosan injection, NFκB protein levels increased in nuclei in SNS Cre-positive, but not in SNS Cre-negative, MYCBP2$^{fl/fl}$ mice (Fig. 10, *E* and *F*). This finding is in accordance with a disturbed Ran-dependent protein export and an accumulation of Ran and its cargo proteins in nuclei.

Finally, we investigated Ran expression in DRGs from SNS Cre-negative and Cre-positive MYCBP2$^{fl/fl}$ mice. As seen for RanGAP1, we found a slight up-regulation of Ran in the absence of MYCBP2 in DRGs of naive mice (Fig. 11*A*). Similar to RanGAP1, Ran expression was not significantly altered in DRGs from SNS Cre-negative MYCBP2$^{fl/fl}$ mice after zymosan injection in one hind paw (Fig. 11*B*). As seen for RanGAP1 (Fig. 2, *D* and *E*), Ran expression significantly increased in the

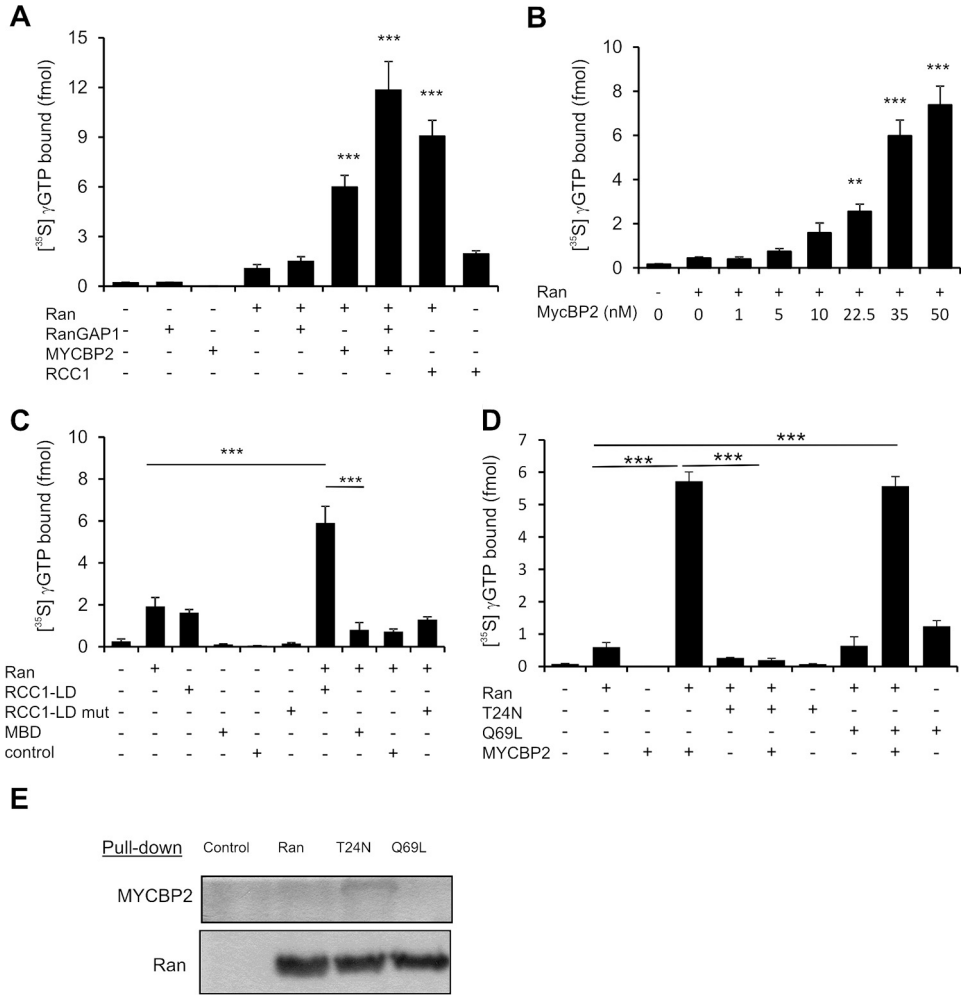

FIGURE 9. **MYCBP2 is a GEF for Ran.** *A,* [^{35}S]GTPγS binding of Ran (2 μM) in the presence of RanGAP1 (100 nM) and/or MYCBP2 (35 nM). RCC1 (35 nM) was used as positive control. Data are presented as mean ± S.E. (n = 3–9). One-way ANOVA/Dunnett's test, ***, $p < 0.001$. *B,* [^{35}S]GTPγS binding of Ran (2 μM) in the presence of increasing MYCBP2 concentration (0–50 nM). Data are presented as mean ± S.E. (n = 3–13). One-way ANOVA/Dunnett's test, **, $p < 0.01$; ***, $p < 0.001$. *C,* [^{35}S]GTPγS binding of Ran in the presence of the RCC1-like domain or an inactive RCC1-like domain or the Myc-binding domain of MYCBP2. Control proteins were obtained by overexpression of an empty TrcHisB vector and subsequent purification. The data are presented as mean ± S.E. (n = 3). One-way ANOVA/Dunnett's test, ***, $p < 0.01$. *D,* [^{35}S]GTPγS binding of Ran (2 μM) in the presence of MYCBP2 (35 nM) and the inactive T24N or the active (Q69L) Ran mutant (6 μM). Data are presented as mean ± S.E. (n = 4). One-way ANOVA/Dunnett's test, ***, $p < 0.001$. *E,* pulldown experiment with purified MYCBP2 and His-tagged Ran, T24N, or Q69L. Proteins were precipitated with nickel-agarose. Western blot analysis was performed using antibodies against MycBP2 in the *upper panel* and against Ran in the *lower panel*. To exclude unspecific binding MYCBP2 was incubated alone with nickel agarose under the same conditions (*control*).

absence of MYCBP2 in DRGs from SNS Cre-positive MYCBP2$^{fl/fl}$ mice 24 h after zymosan injection (Fig. 11*C*). This up-regulation is most likely not due to the absence of ubiquitylation of Ran by MYCBP2, because neither a ubiquitylation-induced shift in the size of Ran was observed nor was MYCBP2 able to ubiquitylate Ran *in vitro* assays (Fig. 11*D*). However, we observed a significant up-regulation of the Ran mRNA levels in DRGs 24 h after zymosan injection (Fig. 11*E*). Therefore, the up-regulation of Ran and RanGAP1 in the absence of MYCBP2 seems to be a compensation for the loss of a functional Ran GTPase cycle.

Discussion

The small GTPase Ran has been shown to regulate nuclear transport, microtubule assembly, nuclear envelope, and nuclear pore complex reformation (2–4) as well as the retrograde transport after traumatic nerve injury (10). Because of the necessity of the presence of a GEF for Ran for retrograde transport, it has been speculated that other GEFs for Ran, besides the nuclear RCC1, might exist. MYCBP2 contains a nuclear localization signal that, together with the fact that it physically interacts with Myc, raised the question about potential functional roles of MYCBP2 in nuclei (13). Here, we describe that MYCBP2 translocation to nuclei is mediated by SUMOylated RanGAP1 and that it acts as GEF for Ran through its RCC1-like domain. The example of MYCBP2 indicates that specialized GEFs for Ran exists that might serve to supplement the role of RCC1 allowing a more complex, cell-specific control of Ran activities.

RanGAP1 is normally located in the cytoplasm but can translocate after SUMOylation to the cytosolic membrane of the nuclear pore complex (40). The translocation of SUMOylated RanGAP1 can also support the transport of other proteins to the nucleus as, for example, shown for the E3 ubiquitin ligase

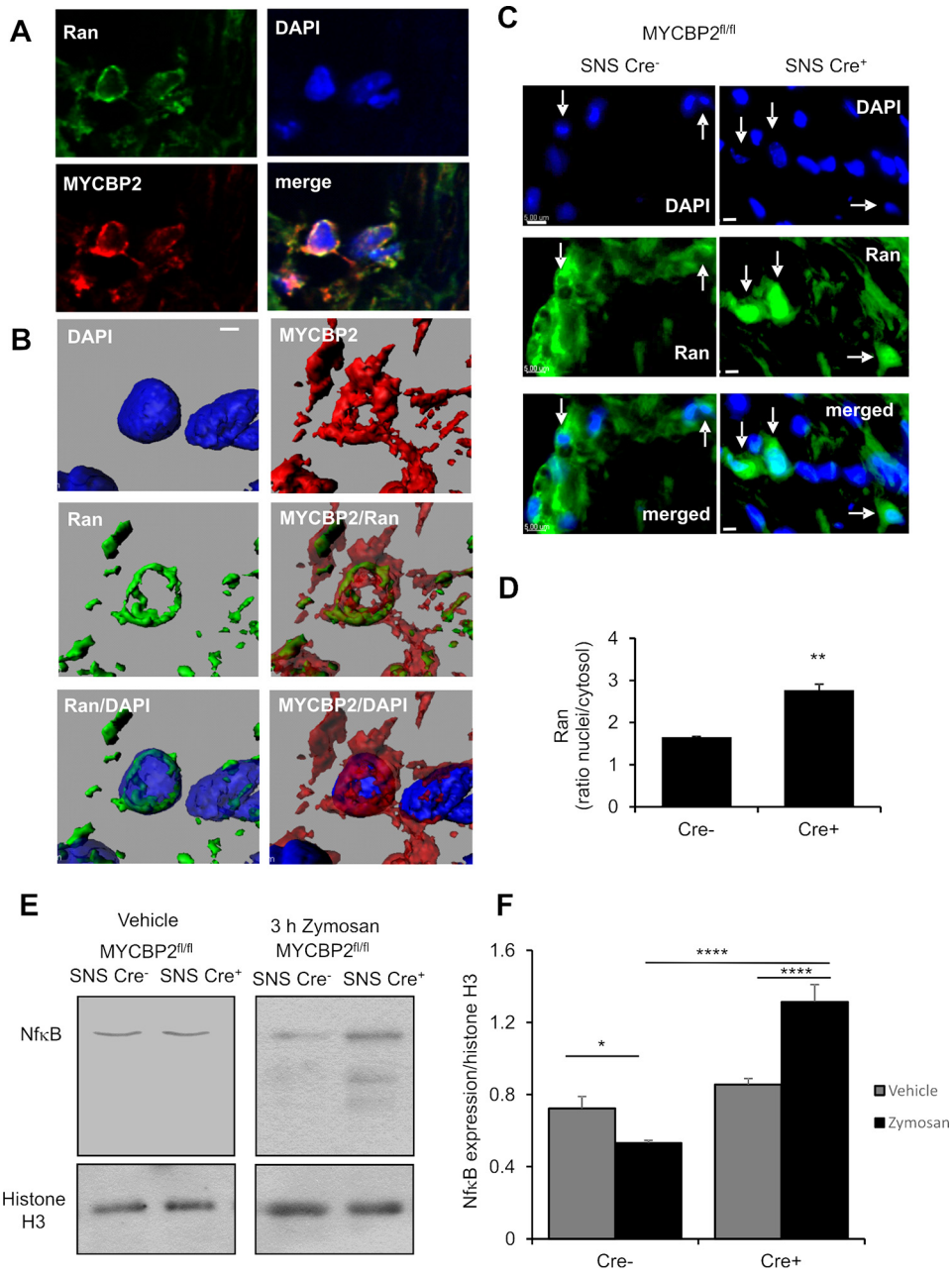

FIGURE 10. **Ran and MYCBP2 are co-localized in nuclei of DRGs.** *A* and *B,* representative immunofluorescence images of one plane of an image stack (*A*) showing DRG neurons of wild type mice were stained for MYCBP2 (*red*), Ran (*green*), and DAPI (*blue*). Three-dimensional reconstruction of the fluorescence images (*B*) using Imaris 7.61. The *white bar* represent 3 μm. *C,* representative images of the Ran localization (*green*) in DRGs from SNS Cre-negative and Cre-positive MYCBP2$^{fl/fl}$. Nuclei were stained with DAPI (*blue*). *Arrows* depict Ran-expressing cells. The *white bar* represents 5 μm. *D,* quantitative evaluation of images as shown in *C* to determine the ratio of nuclear Ran to cytosolic Ran for both genotypes. Data are shown as mean ± S.E. ($n = 50$ cells/group). Student's *t* test, **, $p < 0.01$. *E,* NF-κB expression in nuclei of DRG from SNS Cre-negative and Cre-positive MYCBP2$^{fl/fl}$ mice 3 h after zymosan or vehicle injection. Equal loading was confirmed using histone H3 expression. *F,* densitometric analyses of NFκB expression. Data are shown as mean ± S.E. ($n = 3$ mice). Two-way ANOVA/Bonferroni, *, $p < 0.05$; ****, $p < 0.0001$.

Traf6 (45). We found that MYCBP2 binds selectively to SUMOylated RanGAP1, and that RanGAP1 expression is necessary for the translocation of MYCBP2 to nuclei. The interaction of MYCBP2 to RanGAP1 depends on the presence of SUMO1, because a physical interaction of MYCBP2 and non-SUMOylated RanGAP1 was not detectable. Indeed, a high threshold SUMO-binding motif within MYCBP2 was identified using a SUMO-binding motif recognition program (GPS-SBM 1.0). This SUMO-binding region can either allow MYCBP2 to bind generally to SUMOylated proteins or it can serve to stabilize through SUMO1 binding the interaction between SUMOylated RanGAP1 and MYCBP2. Because immunoprecipitation of MYCBP2 did not yield, except RanGAP1, SUMOylated proteins in detectable amounts, our data point toward a specific interaction of MYCBP2 and SUMOylated RanGAP1. However, we cannot rule out that in other cells or under other conditions additional SUMOylated proteins may bind to MYCBP2. Importantly, down-regulation of RanGAP1 prevented translocation of MYCBP2 to the nucleus suggesting that SUMOylated RanGAP1 functions as a transporter

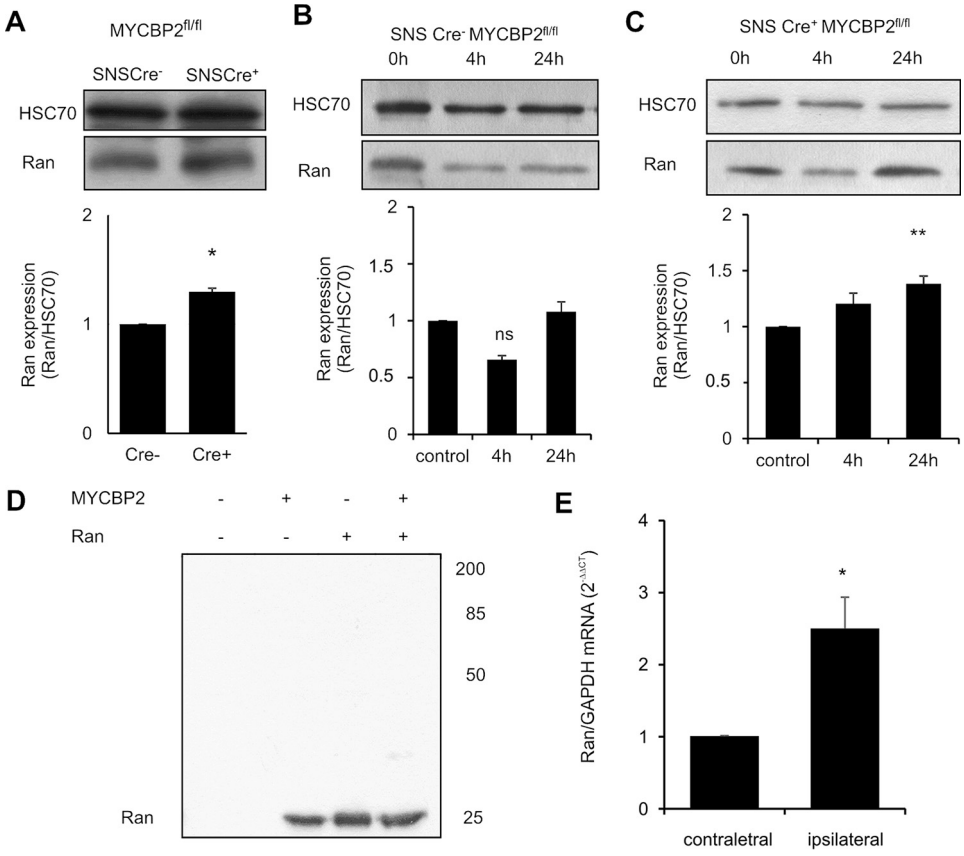

FIGURE 11. **Ran is up-regulated in DRG cells in absence of MYCBP2.** *A,* Ran expression in DRG neurons of SNS Cre-negative and CRE-positive MYCBP2$^{fl/fl}$ mice. Equal loading was confirmed using HCS70 expression. The *lower panel* shows the densitometric analysis of Ran expression. Data are shown as mean ± S.E. ($n = 3$). Two-tailed Student's *t* test, *, $p < 0.05$. *B* and *C,* Ran expression in DRGs from SNS Cre-negative (*B*) and Cre-positive (*C*) MYCBP2$^{fl/fl}$ mice. Expression was tested in naive mice and 4 and 24 h after zymosan injection in one hind paw (20 μl, 12.5 mg/ml). Equal loading was confirmed using HCS70 expression. The *lower panel* shows the respective densitometric analysis. Data are shown as mean ± S.E. ($n = 3$). One-way ANOVA/Dunnett's test, **, $p < 0.01$. *ns*, not significant. *D, in vitro* ubiquitylation assay for MYCBP2 using His-tagged ubiquitin in absence or presence of Ran. The *in vitro* assay was performed in absence of MG132 using purified proteins as described under "Experimental Procedures." The samples were analyzed by Western blot for Ran. *E,* mRNA expression of Ran 24 after zymosan injection compared with control. Data are shown as mean ± S.E. ($n = 3$). Student's *t* test, *, $p < 0.05$.

of MYCBP2. At the same time, SUMOylated RanGAP1 inhibited the ubiquitin ligase activity of MYCBP2, and it is tempting to speculate that SUMOylated RanGAP1 inhibits the ubiquitin ligase activity of MYCBP2 to ensure MYCBP2 silencing during its transport to the nucleus.

Ran is found in high levels in neuronal nuclei but also in the cellular compartments outside of nuclei, indicating cytosolic functions of Ran in neurons (10, 46). GTP- and GDP-bound Ran has been detected in axons of rat sciatic nerve, where GTP-bound Ran is found in a protein complex, including the transport molecules importin-α and dynein. After nerve injury, a local translation increases RanBP1 and RanGAP1 protein levels leading to hydrolysis of Ran-bound GTP and the formation of an importin-α·importin-β·dynein complex enabling retrograde transport of proteins (10). To maintain cytosolic GTP-bound Ran levels in axons of neurons, a cytosolic Ran GEF is necessary. Previously, two GEFs for Ran have been identified, RCC1 and RanBP10. RCC1 is located predominantly in the nucleus, although RanBP10 is highly expressed in the cytosol of megakaryocytes and modulates stability of noncentrosomal microtubules (47). Interestingly, MYCBP2 also mediates its physiological functions toward axon outgrowth and synapse formation by modulating microtubule organization (48), and it can be speculated that MYCBP2/Ran signaling contributes to these effects. A functional interaction of MYCBP2 and Ran in nuclei of neurons is supported by the findings that both proteins co-localize in nuclei and that Ran accumulates in nuclei in the absence of MYCBP2, which can be explained by the reduced ability of Ran to bind GTP and to be exported out of the nucleus. RCC1 is the guanine nucleotide exchange factor for the small GTPase Ran, which consists of seven repeats of a 50–60-amino acid-long motif forming a propeller-like structure. These seven repeats are also present in the RCC1-like domain of MYCBP2 but are interrupted by a 134-amino acid insert after the fourth repeat separating the RCC1-like domain in two elements, RHD-1 and RHD-2 (13). MYCBP2 has been shown to carry a GEF activity for Rheb, although the involvement of its RCC1 domain was not investigated (25). Thus, in accordance with these data, we found that the RCC1-like domain of MYCBP2 carries a GEF activity for the small GTPase Ran.

Evidence for potential involvement of MYCBP2 in the nucleo-cytoplasmic transport has been reported earlier by Grill *et al.* (49). They showed that RPM-1, the ortholog of MYCBP2 in *C. elegans*, binds to RNA Export protein-1 (RAE-1). RAE-1 has in yeast an important role for mRNA export (50). However,

in other organisms it regulates mitotic spindle assembly and cell cycle progression by stabilizing microtubules (51, 52). Grill *et al.* (49) suggested either a role of the MYCBP2/RAE-1 interaction in microtubule organization or nuclear export regulation.

The importance of nuclear transport, and therefore the MYCBP2/Ran interaction, for neuronal functions is evident. Peripheral inflammation induces in sensory neurons activation and nuclear translocation of transcription factors such as NFκB leading to profound transcriptional changes and nuclear export of mRNA or epigenetic regulators such as histone deactylases (31, 41–43). Because stimulation of neurons is necessary to induce the translocation of MYCBP2 to the nucleus, it is not surprising that the strongest effect of the loss of MYCBP2 on Ran and RanGAP1 expression in DRGs is seen after induction of peripheral inflammation. The absence of MYCBP2 causes an up-regulation of Ran and RanGAP1 during inflammatory hyperalgesia, which is, according to our findings, not due to a missing poly-ubiquitylation and a subsequently decreased degradation of both proteins. Instead, we interpret this up-regulation as a compensatory mechanism to reestablish a functional nucleo-cytoplasmic transport, which is reduced due to the decreased GTP-binding ability of Ran.

Taken together, our data show that MYCBP2 and RanGAP1 fulfill opposing roles in the regulation of Ran activity. An especially elegant regulation method is presented by the finding that MYCBP2 transport to the nucleus depends on its counterpart RanGAP1. This way the cell ensures that both regulation partners are present at the nucleus and can control together correct functioning of Ran-dependent transport mechanisms.

Author Contributions—All authors were involved in planning experiments, discussion of the data, and critically revised and approved the manuscript. A. D. contributed the *in vitro* experiments; S. P. generated the constructs; D. D. Z. performed animal experiments; M. H. and S. H. performed the initial experiments in Fig. 1; S. P. and K. S. bred the genetically altered mice. K. S., S. P., and A. D. wrote the manuscript.

References

1. Bischoff, F. R., and Ponstingl, H. (1991) Catalysis of guanine nucleotide exchange on ran by the mitotic regulator RCC1. *Nature* **354,** 80–82
2. Kalab, P., Pu, R. T., and Dasso, M. (1999) The Ran GTPase regulates mitotic spindle assembly. *Curr. Biol.* **9,** 481–484
3. Nagai, M., and Yoneda, Y. (2012) Small GTPase Ran and Ran-binding proteins. *BioMol. Concepts* **3,** 307–318
4. Sazer, S., and Dasso, M. (2000) The Ran decathlon: multiple roles of Ran. *J. Cell Sci.* **113,** 1111–1118
5. Moore, M. S. (1998) Ran and nuclear transport. *J. Biol. Chem.* **273,** 22857–22860
6. Görlich, D., Seewald, M. J., and Ribbeck, K. (2003) Characterization of Ran-driven cargo transport and the RanGTPase system by kinetic measurements and computer simulation. *EMBO J.* **22,** 1088–1100
7. Bischoff, F. R., Klebe, C., Kretschmer, J., Wittinghofer, A., and Ponstingl, H. (1994) RanGAP1 induces GTPase activity of nuclear Ras-related Ran. *Biochemistry* **91,** 2587–2591
8. Mahajan, R., Delphin, C., Guan, T., Gerace, L., and Melchior, F. (1997) A small ubiquitin-related polypeptide involved in targeting RanGAP1 to nuclear pore complex protein RanBP2. *Cell* **88,** 97–107
9. Matunis, M. J., Coutavas, E., and Blobel, G. (1996) A novel ubiquitin-like modification modulates the partitioning of the Ran-GTPase-activating protein RanGAP1 between the cytosol and the nuclear pore complex. *J. Cell Biol.* **135,** 1457–1470
10. Yudin, D., Hanz, S., Yoo, S., Iavnilovitch, E., Willis, D., Gradus, T., Vuppalanchi, D., Segal-Ruder, Y., Ben-Yaakov, K., Hieda, M., Yoneda, Y., Twiss, J. L., and Fainzilber, M. (2008) Localized regulation of axonal RanGTPase controls retrograde injury signaling in peripheral nerve. *Neuron* **59,** 241–252
11. Yudin, D., and Fainzilber, M. (2009) Ran on tracks–cytoplasmic roles for a nuclear regulator. *J. Cell Sci.* **122,** 587–593
12. Ehnert, C., Tegeder, I., Pierre, S., Birod, K., Nguyen, H.-V., Schmidtko, A., Geisslinger, G., and Scholich, K. (2004) Protein associated with Myc (PAM) is involved in spinal nociceptive processing. *J. Neurochem.* **88,** 948–957
13. Guo, Q., Xie, J., Dang, C. V., Liu, E. T., and Bishop, J. M. (1998) Identification of a large Myc-binding protein that contains RCC1-like repeats. *Proc. Natl. Acad. Sci. U.S.A.* **95,** 9172–9177
14. Yang, H., Scholich, K., Poser, S., Storm, D. R., Patel, T. B., and Goldowitz, D. (2002) Developmental expression of PAM (protein associated with MYC) in the rodent brain. *Brain Res. Dev. Brain Res.* **136,** 35–42
15. Bloom, A. J., Miller, B. R., Sanes, J. R., and DiAntonio, A. (2007) The requirement for Phr1 in CNS axon tract formation reveals the corticostriatal boundary as a choice point for cortical axons. *Genes Dev.* **21,** 2593–2606
16. Burgess, R. W., Peterson, K. A., Johnson, M. J., Roix, J. J., Welsh, I. C., and O'Brien, T. P. (2004) Evidence for a conserved function in synapse formation reveals Phr1 as a candidate gene for respiratory failure in newborn mice. *Mol. Cell. Biol.* **24,** 1096–1105
17. D'Souza, J., Hendricks, M., Le Guyader, S., Subburaju, S., Grunewald, B., Scholich, K., and Jesuthasan, S. (2005) Formation of the retinotectal projection requires Esrom, an ortholog of PAM (protein associated with Myc). *Development* **132,** 247–256
18. Schaefer, A. M., Hadwiger, G. D., and Nonet, M. L. (2000) rpm-1, a conserved neuronal gene that regulates targeting and synaptogenesis in *C. elegans*. *Neuron* **26,** 345–356
19. Wan, H. I., DiAntonio, A., Fetter, R. D., Bergstrom, K., Strauss, R., and Goodman, C. S. (2000) Highwire regulates synaptic growth in *Drosophila*. *Neuron* **26,** 313–329
20. Holland, S., Coste, O., Zhang, D. D., Pierre, S. C., Geisslinger, G., and Scholich, K. (2011) The ubiquitin ligase MYCBP2 regulates transient receptor potential vanilloid receptor 1 (TRPV1)-internalization through inhibition of p38 MAPK signaling. *J. Biol. Chem.* **286,** 3671–3680
21. Murthy, V., Han, S., Beauchamp, R. L., Smith, N., Haddad, L. A., Ito, N., and Ramesh, V. (2004) Pam and its ortholog highwire interact with and may negatively regulate the TSC1/TSC2 complex. *J. Biol. Chem.* **279,** 1351–1358
22. Nakata, K., Abrams, B., Grill, B., Goncharov, A., Huang, X., Chisholm, A. D., and Jin, Y. (2005) Regulation of a DLK-1 and p38 MAP kinase pathway by the ubiquitin ligase RPM-1 is required for presynaptic development. *Cell* **120,** 407–420
23. Wu, C., Daniels, R. W., and DiAntonio, A. (2007) DFsn collaborates with Highwire to down-regulate the Wallenda/DLK kinase and restrain synaptic terminal growth. *Neural Dev.* **2,** 16
24. Grill, B., Bienvenut, W. V., Brown, H. M., Ackley, B. D., Quadroni, M., and Jin, Y. (2007) *C. elegans* RPM-1 regulates axon termination and synaptogenesis through the Rab GEF GLO-4 and the Rab GTPase GLO-1. *Neuron* **55,** 587–601
25. Maeurer, C., Holland, S., Pierre, S., Potstada, W., and Scholich, K. (2009) Sphingosine-1-phosphate induced mTOR-activation is mediated by the E3-ubiquitin ligase PAM. *Cell. Signal.* **21,** 293–300
26. Gao, X., and Patel, T. B. (2005) Histidine residues 912 and 913 in protein associated with myc are necessary for the inhibition of adenylyl cyclase activity. *Mol. Pharmacol.* **67,** 42–49
27. Garbarini, N., and Delpire, E. (2008) The RCC1 domain of protein associated with myc (PAM) interacts with and regulates KCC2. *Cell Physiol. Biochem.* **22,** 31–44
28. Scholich, K., Pierre, S., and Patel, T. B. (2001) Protein associated with myc (PAM) is a potent inhibitor of adenylyl cyclases. *J. Biol. Chem.* **276,** 47583–47589

29. Ausubel, F. M., Brent, R., Kingston, R. E., Morre, D. D., Seidman, J. G., Smith, J. A., and Struhl, K. (1987) in *Current Protocols Molecule Biology* (Benson Chanda, V., ed) pp. 10.16.14, John Wiley & Sons, Inc., New York
30. Pierre, S., Maeurer, C., Coste, O., Becker, W., Schmidtko, A., Holland, S., Wittpoth, C., Geisslinger, G., and Scholich, K. (2008) Toponomics analysis of functional interactions of the ubiquitin ligase PAM (protein associated with myc) during spinal nociceptive processing. *Mol. Cell. Proteomics* **7,** 2475–2485
31. Niederberger, E., and Geisslinger, G. (2010) Analysis of NF-κB signaling pathways by proteomic approaches. *Expert Rev. Proteomics* **7,** 189–203
32. Melchior, F., Sweet, D. J., and Gerace, L. (1995) Analysis of Ran/TC4 function in nuclear protein import. *Methods Enzymol.* **257,** 279–291
33. Gama, L., and Breitwieser, G. E. (1999) Generation of epitope-tagged proteins by inverse PCR mutagenesis. *BioTechniques* **26,** 814–816
34. Talcott, B., and Moore, M. S. (2000) The nuclear import of RCC1 requires a specific nuclear localization sequence receptor, Karyopherin α3/Qip. *J. Biol. Chem.* **275,** 10099–10104
35. Zou, C., Ellis, B. M., Smith, R. M., Chen, B. B., Zhao, Y., and Mallampalli, R. K. (2011) Acyl-CoA:lysophosphatidylcholine acyltransferase I (Lpcat1) catalyzes histone protein *O*-palmitoylation to regulate mRNA synthesis. *J. Biol. Chem.* **286,** 28019–28025
36. Kehlenbach, R. H., Assheuer, R., Kehlenbach, A., Becker, J., and Gerace, L. (2001) Stimulation of nuclear export and inhibition of nuclear import by a ran mutant deficient in binding to ran-binding protein 1. *J. Biol. Chem.* **276,** 14524–14531
37. Kehlenbach, R. H., Dickmanns, A., Kehlenbach, A., Guan, T., and Gerace, L. (1999) A role for RanBP1 in the release of CRM1 from the nuclear pore complex in a terminal step of nuclear export. *J. Cell Biol.* **145,** 645–657
38. Scholich, K., Mullenix, J. B., Wittpoth, C., Poppleton, H. M., Pierre, S. C., Lindorfer, M. A., Garrison, J. C., and Patel, T. B. (1999) Facilitation of signal onset and termination by adenylyl cyclase. *Science* **283,** 1328–1331
39. Qiao, X., Pham, D. N., Luo, H., and Wu, J. (2010) Ran overexpression leads to diminished T cell responses and selectively modulates nuclear levels of c-Jun and c-Fos. *J. Biol. Chem.* **285,** 5488–5496
40. Pichler, A., and Melchior, F. (2002) Ubiquitin-related modifier SUMO1 and nucleocytoplasmic transport. *Traffic* **3,** 381–387
41. Schlumm, F., Mauceri, D., Freitag, H. E., and Bading, H. (2013) Nuclear calcium signaling regulates nuclear export of a subset of class IIa histone deacetylases following synaptic activity. *J. Biol. Chem.* **288,** 8074–8084
42. Pierre, S., Eschenhagen, T., Geisslinger, G., and Scholich, K. (2009) Capturing adenylyl cyclases as potential drug targets. *Nat. Rev. Drug Discov.* **8,** 321–335
43. von Hehn, C. A., Baron, R., and Woolf, C. J. (2012) Deconstructing the neuropathic pain phenotype to reveal neural mechanisms. *Neuron* **73,** 638–652
44. Nakagawa, K., and Kuzumaki, N. (2005) Transcriptional activity of megakaryoblastic leukemia 1 (MKL1) is repressed by SUMO modification. *Genes Cells* **10,** 835–850
45. Pham, L. V., Zhou, H.-J., Lin-Lee, Y.-C., Tamayo, A. T., Yoshimura, L. C., Fu, L., Darnay, B. G., and Ford, R. J. (2008) Nuclear tumor necrosis factor receptor-associated factor 6 in lymphoid cells negatively regulates c-Myb-mediated transactivation through small ubiquitin-related modifier-1 modification. *J. Biol. Chem.* **283,** 5081–5089
46. Sepp, K. J., Hong, P., Lizarraga, S. B., Liu, J. S., Mejia, L. A., Walsh, C. A., and Perrimon, N. (2008) Identification of neural outgrowth genes using genome-wide RNAi. *PLoS Genet.* **4,** e1000111
47. Schulze, H., Dose, M., Korpal, M., Meyer, I., Italiano, J. E., Jr., and Shivdasani, R. A. (2008) RanBP10 is a cytoplasmic guanine nucleotide exchange factor that modulates noncentrosomal microtubules. *J. Biol. Chem.* **283,** 14109–14119
48. Lewcock, J. W., Genoud, N., Lettieri, K., and Pfaff, S. L. (2007) The ubiquitin ligase Phr1 regulates axon outgrowth through modulation of microtubule dynamics. *Neuron* **56,** 604–620
49. Grill, B., Chen, L., Tulgren, E. D., Baker, S. T., Bienvenut, W., Anderson, M., Quadroni, M., Jin, Y., and Garner, C. C. (2012) RAE-1, a novel PHR binding protein, is required for axon termination and synapse formation in *Caenorhabditis elegans*. *J. Neurosci.* **32,** 2628–2636
50. Brown, J. A., Bharathi, A., Ghosh, A., Whalen, W., Fitzgerald, E., and Dhar, R. (1995) A mutation in the *Schizosaccharomyces pombe rae1* gene causes defects in poly(A)$^+$ RNA export and in the cytoskeleton. *J. Biol. Chem.* **270,** 7411–7419
51. Babu, J. R., Jeganathan, K. B., Baker, D. J., Wu, X., Kang-Decker, N., and van Deursen, J. M. (2003) Rae1 is an essential mitotic checkpoint regulator that cooperates with Bub3 to prevent chromosome missegregation. *J. Cell Biol.* **160,** 341–353
52. Wong, R. W., Blobel, G., and Coutavas, E. (2006) Rae1 interaction with NuMA is required for bipolar spindle formation. *Proc. Natl. Acad. Sci. U.S.A.* **103,** 19783–19787